2012

GROUP I METABOTROPIC GLUTAMATE RECEPTORS ON SELECTIVE CELLULAR SUBTYPES IN EPILEPTOGENIC MALFORMED CORTEX

William Bruch
Virginia Commonwealth University

COPYRIGHT PAGE

GROUP I METABOTROPIC GLUTAMATE RECEPTORS ON SELECTIVE CELLULAR SUBTYPES IN EPILEPTOGENIC MALFORMED CORTEX

A thesis submitted in partial fulfillment of the requirements for the degree of Master of Science at Virginia Commonwealth University.

By

William Mark Bruch III
Post-Baccalaureate Graduate Certificate in
Pre-Medical Basic Health Sciences, 2010
Bachelor of Science, Wake Forest University, 2009

Virginia Commonwealth University
Richmond, Virginia
June, 2012

ACKNOWLEDGMENT

I would like to thank Dr. Kimberle Jacobs for her assistance and guidance over the past years. I would also like to thank my committee members: Dr. Babette Fuss, and Dr. Dong Sun for their suggestions and time. I would like to thank Dr. Scott Henderson and Frances White for their assistance with the Leica TCS-SP2 AOBS microscope and software. I would also like to thank fellow lab member Makoto Ezure and former lab members Anthony Pomicter and Dr. Andrew Bell for being valuable resources and perpetually helpful. Lastly, I would like to thank my parents for being supportive through this process.

TABLE OF CONTENTS

LIST OF FIGURES

ABSTRACT

GROUP I METABOTROPIC GLUTAMATE RECEPTORS ON SELECTIVE CELLULAR SUBTYPES IN EPILEPTOGENIC MALFORMED CORTEX

By William M. Bruch

A thesis submitted in partial fulfillment of the requirements for the degree of Master of Science at Virginia Commonwealth University.

Virginia Commonwealth University, 2012

Advisor: Kimberle M. Jacobs, Ph.D.
Associate Professor, Department of Anatomy and Neurobiology

Cortical malformations from altered development are common causes of human epilepsy. The cellular mechanisms responsible for the epileptic state of cortex remain unclear and a significant portion of these cases do not respond to treatment. Previous electrophysiological recordings in the Jacobs lab in a rat polymicrogyria model indicated an increased response to group I metabotropic glutamate receptor agonists in the region adjacent to the malformation (PMZ). In addition there was a novel response in low threshold spiking (LTS) interneurons via mGluR5 activation. To determine whether cell specific expression of these receptors was altered in malformed cortex immunohistochemical stains were performed for group I mGluRs along with non-overlapping interneuron subtype specific markers, a neuronal marker and general inhibitory cell marker. There was no altered mGluR5 expression seen in the PMZ. There was an altered expression seen in PMZ mGluR1α labeled cells and cells in other cortical regions.

CHAPTER 1

INTRODUCTION

1.1 Thesis Overview:

A significant proportion of intractable epilepsies are associated with developmental cortical malformations. The difficulty in treating this type of epilepsy is due in part to the fact that the cellular mechanisms that contribute to the hyperexcitable state of malformed cortex are not fully understood. The Jacobs lab has been determining the contribution of group I metabotropic glutamate receptors ($mGluR_I$) to epileptogenic cortex using a known animal model for the human cortical developmental malformation, polymicrogyria. Interneurons in microgyric cortex show an increased responsiveness to $mGluR_I$ agents, and therefore represent a potential target in the development of novel antiepileptic drugs. In evaluating the efficacy of group I antagonists for pharmaceutical applications, the cell specific expression of these receptors is relevant to potential side effects and the mechanism of action. The goal of this project was to determine whether there is a difference in the subtype of cells expressing $mGluR_I$ immunoreactivity in microgyric compared to normal rat cortex.

1.2 Epilepsy:

Epilepsy is one of the most common neuronal brain disorders, affecting at least fifty million people worldwide (World Federation of Neurology et al., 2005). Epilepsy, defined as recurrent unprovoked seizures, is a debilitating condition that has great implications on the lives of those affected. These patients have difficulty with maintaining a driver's license, relationships, social isolation, employment and educational opportunities (World Federation of Neurology et al., 2005). Epilepsy can be seen as an umbrella term that encompasses a vast array of underlying etiologies that ultimately lead to an increased propensity for synchronized neuronal activity within the brain (Beck and Elger, 2008).

1.3 Treatment/prognosis and introduction to cortical malformations (clinical):

The majority of patients with epilepsy respond to treatment with antiepileptic drugs (AEDs), however, 30-40% of patients continue to experience recurrent seizures despite attempted drug treatments (Kwan and Brodie, 2006). Cortical malformations denote a major cause of epilepsy (Guerrini and Carrozzo, 2002). Non-pharmacological treatment options for refractory cases include surgery, vagal nerve stimulation and ketogenic diets (World Federation of Neurology et al., 2005). However, these treatments are only effective in a minority of malformation-associated epilepsy patients.

Surgical resection has proved to be a successful treatment option when the seizure origin is located, and restricted to either a focal region or one hemisphere (Blumcke et al., 2009; Sisodiya, 2000). However, surgical success has been limited in epilepsies stemming from malformations of cortical development with only around 40% of patients remaining seizure free two years after surgery (Sisodiya, 2000). This limited success rate can be attributed to factors including: limited EEG and ECoG spatial resolution in delineating the epileptogenic zone, and the potential for widespread abnormalities extending beyond the localized epileptogenic region of cortex (Sisodiya, 2000). A specific example of epilepsy resulting from a malformation of cortical development that likely has limited potential for surgical treatment is polymicrogyria (Sisodiya, 2004).

1.4 Polymicrogyria Background

Polymicrogyria is one of the most common malformations of cortical development, and can often be identified through magnetic resonance imaging by the presence of excessive abnormal cortical gyrations (Barkovich, 2010; Sisodiya, 2004). Occasionally there is fusion of

the overlying molecular layer resulting in an absence of visible gyri on the exterior of the cortex (Sisodiya, 2000). There are two defined histological presentations of this malformation consisting of either unlayered or four layered cortex. Unlayered polymicrogyria is caused by an early disruption of neuronal migration and results in an external molecular layer that does not follow the normal pattern of convolutions, and underlying neurons that lack laminar organization (Guerrini and Carrozzo, 2002). Four layered polymicrogyria, as the name suggests, is identified by the presence of four cortical layers instead of the six layers seen in normal cortex (Guerrini and Filippi, 2005). This layering pattern is consistent with a brain that has suffered an insult between the twentieth and twenty-fourth week of gestation (Guerrini and Carrozzo, 2002). Causes that have been linked to polymicrogyria have been genetic mutations, congenital infections, localized or diffuse in utero ischemia, and abdominal trauma during pregnancy (Barkovich, 2010; Montenegro et al., 2002). These events ultimately lead to a death of the deep cortical layers, as evidenced by the presence of a layer of intracortical laminar necrosis (Guerrini and Filippi, 2005; Montenegro et al., 2002). This is due to the idea that an insult during this early stage of development will specifically affect the deep layers which will be within the cortical plate, as the brain is developing in an inside out manner (Rakic and Lombroso, 1998).

Clinical presentations of polymicrogyria can be focal, regional, hemispheric, or involve the entire cortical mantle (Guerrini and Carrozzo, 2002; Sisodiya, 2004). Affected individuals exhibit differing levels of symptoms ranging from mild cognitive impairments to severe encephalopathy, spastic paresis and intractable epilepsy (Araujo et al., 2006; Guerrini and Carrozzo, 2002). Surgery for polymicrogyria patients with intractable epilepsy has proved difficult, as the epileptogenic networks have been shown to extend well beyond the visible lesion even in cases of focal polymicrogyria (Chassoux et al., 2008). Neurons within the malformation

have also been shown to be functional, which has hindered surgical success/options in cases where the epileptic zone includes areas of eloquent cortex (Araujo et al., 2006). Alternative treatment options are necessary, however, given the fact that polymicrogyria remains poorly understood there are currently limited options for many individuals who consequently lead a severely debilitated life. (Columbo 2009-for the poorly understood)

1.5 Animal Model

The Dvorak lab developed an animal model for four-layered microgyria in rats by inducing a hypoxic event. This is accomplished by focal contact freezing: applying a probe, cooled to negative one hundred degrees Celsius, to a rat's exposed skull at birth for one to two and a half seconds. Rats are born at an early stage of development, which is equivalent to the eighteen to twenty-fourth gestational weeks in humans (Dvorak and Feit, 1977; Humphreys et al., 1991). This time period occurs before the completion of neuronal migration with part of layer IV being the outermost cortical layer at birth. Focal contact freezing at this time causes thrombosis of the blood vessels and necrosis of layers IV, V and Via (Dvorak and Feit, 1977). The necrosis of these layers leaves a glial scar, however, this scar does not halt neuronal migration as capillaries and neuroblasts destined for the I-III cortical layers survive and layer accordingly (Dvorak and Feit, 1977). Layer VIb survives due to its reliance on the subcortical vascular network, whereas the area of necrosis was reliant on pial blood vessels (Dvorak and Feit, 1977; Humphreys et al., 1991). The resulting layering histologically resembles a human four-layered microgyrus: layer 1 is continuous with the molecular layer of the adjacent normal six layered cortex, layer 2 consists of layer II/III neurons and is contiguous with the adjacent layer II/III, layer 3 is mostly a glial scar, and layer 4 consists of the persistent portion of layer VIb (Dvorak and Feit, 1977; Humphreys et al., 1991; Jacobs et al., 1996; Rosen et al., 1996) .

This layering pattern is histologically similar to that seen in human cases of polymicrogyria (Dvorak et al., 1978). Typical six layered cortex resumes at distances of 300-500 micrometers from the microsulcus (Jacobs et al., 1996). This model is significant in that it presents the idea that the aberrant layering seen in polymicrogyria is the result of an event that occurs in a time-specific manner during neuroblast migration. Dvorak was able to demonstrate this by replicating this experiment using rat pups that were four days postnatal. By the forth postnatal day neuronal migration is coming to an end in rat cortex (Dvorak et al., 1978). When focal contact freezing was attempted at this age, the microgyric malformation did not form (Dvorak et al., 1978).

Neurons located in and adjacent to the microsulcus appear to be morphologically normal when Nissl stains are applied to sections from animals perfused at postnatal days 21 and 60 (Humphreys et al., 1991). However neurofilament, GFAP and glutamate stains reveal widespread disruption of neocortical architecture (Humphreys et al., 1991). Neurofilment staining is devoid in the area of the microgyrus while adjacent cortex exhibits increased staining in comparison to control cortex (Humphreys et al., 1991). This increase can be explained by either an increase in the sprouting of axodendritic processes or from the preservation of processes that would otherwise be eliminated. This could suggest an overabundance of excitatory input (Humphreys et al., 1991). Staining of glutamatergic processes also suggests there is a diminution of glutamatergic processes in the zone of neuronal loss and in adjacent layer VIb, as well as distorted placement and orientation of glutamatergic processes in layer V of the zones immediately adjacent to the area of neuronal loss (Humphreys et al., 1991).

Clinical presentations of polymicrogyria are often associated with epilepsy (Barkovich, 2010). Similar physiological abnormalities can be seen in the Dvorak model. Cortex in this model exhibits a focal hyperexcitable region adjacent to the microsulcus as early as postnatal day

12 and is seen in rats as old as postnatal day 118 (animals older than P118 were not analyzed) (Jacobs et al., 1996). This hyperexcitability was evoked in vitro in cortical brain slices at distances one to two millimeters away from the microsulcus and was seen as variable latency multiphasic events characterized as epileptiform (Jacobs et al., 1996). This focal region of hyperexcitability is referred to as the paramicrogyral zone (PMZ) and consists of normal six-layered cortex, which typically resumes at a distance of 300-500 micrometers from the microsulcus (Jacobs et al., 1996). Surgical resection of the microsulcus had no effect on the hyperexcitable state of the paramicrogyral zone (Prince et al., 1997).

A hypothesis for these observations is that afferents originating from cortical and extracortical sites lose their targets in the microgyrus and make laminar contacts in the adjacent cortex (Jacobs et al., 1999b). Interestingly, at the time period when the epileptogenic activity is first seen in the cortex there is a reduction in the number of immunoreactive cells in a specific interneuron subpopulation, however, there appears to be a lack of reduction in inhibition in electrophysiological recordings (Jacobs and Prince, 2005). This may be due to compensatory sprouting and reorganization of surviving interneurons or increased afferent excitatory inputs on interneurons (Jacobs and Prince, 2005).

1.6 Interneurons:

Interneurons account for 20-30% of total neocortical neurons (Markram et al., 2004). Despite sharing the common trait of mostly being inhibitory cells they exhibit a diverse array of morphological, physiological, molecular and synaptic characteristics (Markram et al., 2004). Efforts have been made to classify interneurons into distinct subgroups based on each of these characteristics, but these classifications have often differed amongst labs. A group was recently

formed called the Petilla interneuron nomenclature Group or PING to define universally accepted terms for use in describing the anatomical, physiological and molecular features of GABAergic interneurons of the cerebral cortex (Ascoli et al., 2008). Ideally a classification will account for all three features; however, this is not always feasible.

The distinguishing feature of interneurons is that their axon does not leave the cortex. They usually arborize within a column or are capable of projecting laterally between columns; however they do not project down into the white matter or to distant brain regions (Markram et al., 2004). Most interneurons receive both excitatory and inhibitory synapses on their somata. Different types of inhibitory neurons seem to be specific in their targeting of different neuronal subdomains: dendritic, versus axonal or somal (Markram et al., 2004). Inhibitory interneurons are capable of changing action potential discharge phasing and synchronizing neuronal activity (Markram et al., 2004). This allows them to play a crucial role in the maintenance of the balance between excitation and inhibition.

Alterations in inhibitory circuits are capable of creating hyperexcitable cortex and are believed to be responsible for some of the clinical features of psychological disorders such as Schizophrenia, autism and intellectual disabilities (Dichter and Ayala, 1987; Marin, 2012). There are two functionally distinct inhibitory networks in cortex: fast spiking (FS), and low threshold spiking LTS) neurons (Gibson et al., 1999). These two networks are comprised of interneurons that exhibit characteristic electrophysiological properties. FS interneurons fire distinct repetitive discharges at depolarizing potentials with almost no adaptation, whereas LTS interneurons demonstrate burst firing from a hyperpolarized state with adaptation (Kawaguchi, 1993). Interneurons of the same type are strongly interconnected through electrical synapses (FS with FS, and LTS with LTS), allowing for the synchronization of spikes amongst coupled

interneurons (Beierlein et al., 2000; Gibson et al., 1999). Interneurons within each of these networks share certain morphological and histological characteristics that allow for further classification (Gibson et al., 1999; Kawaguchi and Kondo, 2002; Kawaguchi and Kubota, 1993).

Morphological classifications of interneurons include: large basket cells, small basket cells, nest basket cells, chandelier cells, Martinotti cells, bipolar cells, double bouquet cells, bitufted cells, and neuroglia form cells (Markram et al., 2004). In rat cortex FS interneurons are multipolar neurons and have been identified as basket cells and chandeleir cells. (Kawaguchi 1993 and Kawaguchi 1997) The calcium binding protein PValbumin (PV) is used histologically as a marker for FS cells (Kawaguchi and Kubota, 1993). Biocytin injections in PV cells reveal denser axonal branches near the somata and axons that extend in a horizontal direction (Kawaguchi and Kubota, 1993). In addition, these cells are known to provide powerful inhibition that creates horizontal focally regions of excitation. LTS cells appear to encompass both multipolar and bitufted interneurons, but typically extend their axons vertically to layer I and occasionally downwards to deeper layers (Kawaguchi, 1993). Vasointestinal Protein (VIP) and Somatostatin (SS) are used as non-overlapping histological markers and label non-FS inerneurons; VIP primarily labels double bouquet cells while SS primarily labels Martinotti cells (Kawaguchi and Kubota, 1997). Both of these cell types typically have processes only within one column, but between layers, thus they provide interlaminar, intracolumnar inhibition.

In the freeze lesion rat model of polymicrogyria alterations have been observed in interneuron development as well as their intrinsic properties (George and Jacobs, 2011; Jacobs et al., 1996; Prince et al., 1997; Rosen et al., 1998). At immature rat ages PV neuronal and neuropil staining is diminished within the microgyrus and the adjacent paramicrogyral zone compared to control cortex, however, this is a transient reduction that reaches control levels as the rat ages in

all regions except for layers IV and V immediately adjacent to the microgyrus (Jacobs et al., 1996; Prince et al., 1997; Rosen et al., 1998). Electrophysiological recordings from rats aged postnatal day (P)12-17 indicate a potential increase in the efficacy of LTS cells and a simultaneous decrease in the efficacy of FS cells within the paramicrogyral zone (George and Jacobs, 2011).

Epileptiform activity can result from decreased inhibition (Dichter and Ayala, 1987). In an effort to determine whether this mechanism could explain the epileptiform activity seen in the PMG model a number of labs have performed cell counts of immunohistochemically labeled GABA and GABA subtype markers. Schwarz et al performed counts on GABA-labeled cells and found no change in malformed cortex (Schwarz et al., 2000). They also counted PV-labeled cells and found no difference (Schwarz et al., 2000). In contrast Rosen et al found an initial decrease throughout the malformed area that was a complete change in the pattern of PV staining (Rosen et al., 1998). The reduction in malformed cortex was transient and recovered by P21 (Rosen et al., 1998). However, there remained a persistent selective decrease of around ~20% in cell counts within the deep layers adjacent to the microgyrus, as well as, a loss within the microgyrus itself (Rosen et al., 1998).

There were two significant differences between the methods employed by Schwarz and Rosen. The first difference was in the age of the animals studied which was much older in the Schwarz study (two to four months old). Secondly, all cells from the pia to white matter were counted in the Schwarz study. This may have masked the specific deep layer result determined in the Rosen study (Intro Fig A).

One change that was observed by the Schwarz group was an increase in cells that labeled for the marker calbindin. Calbindin is found in interneurons that label for PV and SS(Kawaguchi and Kubota, 1997). Since a decrease was already found in the PV interneurons, the increase in calbindin was suspected to be due to an increase in the number of SS interneurons. However, a study by Connors that specifically looked only in the deep layers adjacent to the microgyrus (Intro Fig A), found no difference in the number of SS-labeled neurons (Patrick et al., 2006). The Jacobs lab has also recently conducted stereological counts for PV, SS and VIP markers (unpublished Ezure and Jacobs). These counts did reveal selective increases in SS labeling in regions distinct from those analyzed by Patrick et al. An increase was seen in SS labeling within the microgyrus and in layer IV 2.2 mm lateral of the microgyrus. A simultaneous reduction was seen in PV labeling in these regions, which coincided with no overall change in glutamate decarboxylase (GAD) labeling (Intro Fig B). GAD is a marker for GABAergic cells. These results suggest that there is a differential effect seen in these two interneuron subtypes in PMG cortex. This very well may be due to a cortical compensation for the loss of PV neurons by an increase in the SS neurons.

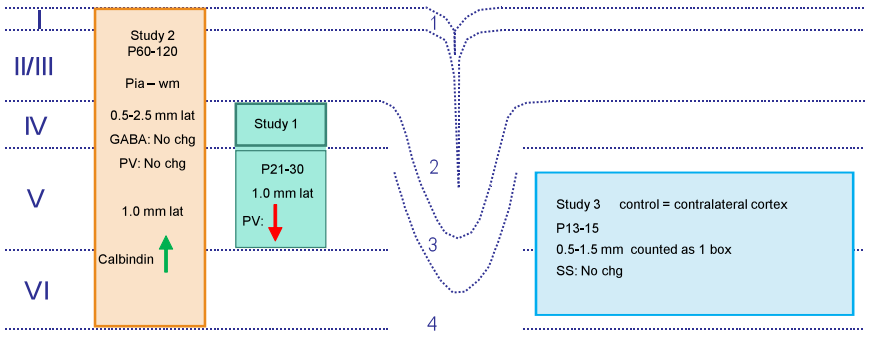

Study 1: Rosen, Jacobs & Prince 1998 Cerebral Cortex, 8: 753-761.
Study 2: Schwarz, Stichel & Luhmann 1998 Epilepsia, 41: 781-787.
Study 3: Patrick, Connors & Landisman 2006 Epilepsy Research, 70: 161-171.

Intro Fig A: Summary figure of previous immunohistochemical studies in the freeze lesion model of PMG in rat cortex. The microgyrus and its layers (1-4) can be seen in the middle of the figure and adjacent cortex with normal six layering (I-VI) can be seen on either side. Box placement indicates the location and relative size of the region analyzed in each study. Study 1 shows findings from Rosen et al. as well as Prince and Jacobs. They looked in the deep layers in the region 1 mm lateral of the microgyrus in rats at P21-30 and saw a reduction in PV labeling. Study 2 was conducted by Schwarz et al. in 2-4 month old rats. They counted from pia to white matter and saw no change in GABA or PV labeling, but did see an increase in calbindin labeled cells. Patrick et al. conducted a study in rats at P13-15, focusing in the deep layers of the region adjacent to the microgyrus. They looked in a wider region spanning from 0.5 mm-1.5 mm lateral to the microgyrus. They looked at SS labeling and saw no change.

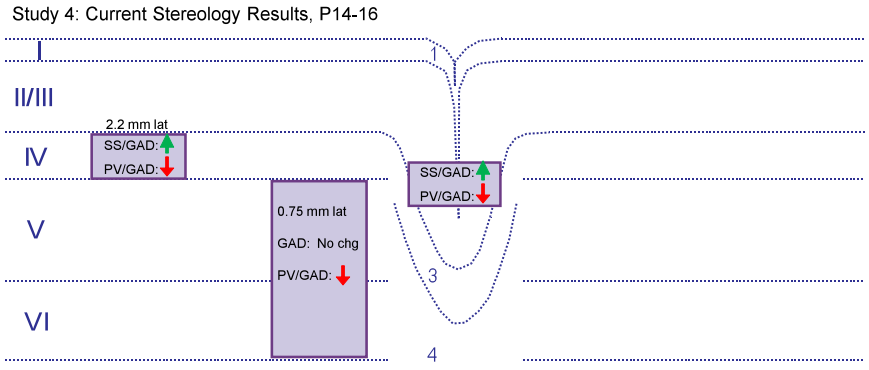

Intro Fig B: Summary figure of unpublished results from stereological counts conducted by the Jacobs lab. This study was conducted in rats at P14-16. Previous findings were confirmed: that there is a decrease seen in PV labeling in the deep layers adjacent to the malformation, as well as, no change in GAD labeling. The most interesting part of the stereology findings is that at two locations (within the microgyrus and layer IV 2.2 mm lateral to the microgyrus) there is a selective increase in SS labeling relative to GAD and a simultaneous decrease in PV labeling relative to GAD. There is no overall change in GAD labeling, however, there is a differential effect on these two interneuron sub types.

1.7 Group I Metabotropic Glutamate Receptors

Metabotropic glutamate receptors are a heptahelical rector family of G protein coupled receptors that are currently divided into three groups based on sequence homology, transduction mechanisms and pharmacological properties (Pin and Bockaert, 1995; Tang et al., 2009). Group I consists of mGluR subunits 1 and 5, group II includes subunits 2 and 3, and group III is

comprised of subunits 4,6,7, and 8 (Tang et al., 2009). Group I mGluRs are primarily located postsynaptically while groups II and III are mostly presynaptic with the exception of mGluR6 which is located postsynaptically in 'ON' bipolar cells of the retina (Tang et al., 2009). Both Group I receptors activate phospholipase C which causes an increase in diacylglycerol and inositoltriphosphate (Deng et al., 2004; Pin and Bockaert, 1995). These increases activate protein kinase C which initiates an increase in intracellular calcium levels (Deng et al., 2004). In contrast, receptors from groups II and III are negatively coupled to adenylyl cyclase (Pin and Bockaert, 1995). Group I mGluRs have been shown to play a crucial role in cortical organization and synaptic modulation (Ballester-Rosado et al., 2010). They have also been identified as potential therapeutic targets for an assortment of neurological disorders including: epilepsy, Fragile X Syndrome, and Parkinson's Disease (Bear et al., 2004; Benarroch, 2008).

The organizational role that mGluR5 receptors play in somatosensory cortex was determined through the creation of a mouse line that specifically knocked out mGluR5 expression in excitatory cortical neurons (Ballester-Rosado et al., 2010). The cortical maps in these animals developed abnormally with disrupted barrel formation and thalamacortical afferent (TCA) patterning (Ballester-Rosado et al., 2010). Layer IV cortical neurons fail to cluster into barrel walls and the TCAs are seen as diffuse patches (Ballester-Rosado et al., 2010). Eliminating mGluR5 from cortical glutamatergic neurons also affects the GABAergic network. A reduction in GABAergic inputs is seen in layer IV neurons in these mice (Ballester-Rosado et al., 2010). Additionally reduction of mGluR5 has been shown to correlate with a reduction in spine density in layer IV spiny neurons (Ballester-Rosado et al., 2010; Wijetunge et al., 2008). Group I mGluRs in the CA1 region of the hippocampus also play an active role in the organization of neuronal circuits through synaptic plasticity.

One example of group I's role in synaptic plasticity is their involvement in long-term potentiation (LTP) and long-term depression (LTD) in the CA1 region of the hippocampus (Mellentin et al., 2006; Neyman and Manahan-Vaughan, 2008). When the mGluR5 antagonist MPEP was administered before high frequency tetani (HFT) both the induction and late phases of LTP were inhibited (Neyman and Manahan-Vaughan, 2008). When MPEP was administered after HFT late phases of LTP were still inhibited (Neyman and Manahan-Vaughan, 2008). MPEP administered before LFS, impaired but did not prevent the induction of LTD (Neyman and Manahan-Vaughan, 2008). Applying MPEP after LFS also significantly impaired the late phases of LTD. The application of the mGluR5 agonist CHPG converts short-term depression into LTD through the activation of protein synthesis (Neyman and Manahan-Vaughan, 2008). The mGluR1 antagonist LY367385 impaired the induction and late phases of both LTD and LTP when applied before LFS and HFT, and had no affect when applied after LFS or HFT (Neyman and Manahan-Vaughan, 2008). The activation of group I mGluRs likely triggers protein synthesis that is necessary for the persistence of synaptic plasticity (Neyman and Manahan-Vaughan, 2008). Disruption of this mechanism has been implicated in fragile X syndrome.

The Group I mGluR signaling pathway is altered in a model of fragile X syndrome and has been identified as a possible mechanism for the disorder (Bear et al., 2004; Huber et al., 2002). This syndrome is caused by a mutation in the Fmr1 gene that encodes fragile x mental retardation protein (FMRP) (Huber et al., 2002). Group I mGluR activation has been shown to increase the production of FMRP near the synapses (Weiler et al., 1997). FMRP associates with the translation machinery and halts further mGluR activated protein synthesis through an end product inhibition mechanism (Bear et al., 2004; Weiler et al., 1997). This pathway is the manner in which LTD is achieved in the hippocampus and is selectively enhanced in Fmr1 knockout

mice, which lack FMRP (Huber et al., 2002). This has led to the theory that the neurological and psychiatric aspects of fragile X syndrome stem from exaggerated LTD, which may account for slowed synaptic maturation (Bear et al., 2004). Group I mGluRs have been proposed as therapeutic targets for the treatment of this syndrome (Bear et al., 2004). Both FMRP and group I mGluRs are widely expressed throughout the brain, which may mean that exaggerated group I mGluR driven protein synthesis accounts for other key features of fragile x syndrome (Bear et al., 2004).

Fragile X syndrome is associated with an increased incidence of epilepsy (Bear et al., 2004). The mGluR5 antagonist MPEP has been shown in other instances to have anticonvulsant applications (Borowicz et al., 2009). Combining MPEP with subprotective doses of conventional antiepileptic drugs shortened seizure duration and after seizure discharge duration for amygdala kindled seizures (Borowicz et al., 2009). Group I agonists have been shown to be capable of inducing synchronized spiking activity in the LTS interneuron networks via electric coupling amongst LTS cells (Beierlein et al., 2000). This synchronization induces a synchronized inhibition in RS and FS neurons, which can be seen over a distance of several hundred microns (Beierlein et al., 2000). The involvement of group I mGluRs in the ability of LTS cells to coordinate the firing pattern of most cortical neurons makes them a particular area of interest in the search for underlying mechanisms in hyper excitable cortex. Synchronous activity among LTS cells appears abruptly in rats between P12-15, which overlaps with the onset of active somatosensory exploration (Long et al., 2005). This timing coincides with the developmental period that the cortex begins to exhibit a hyperexcitable state in the rat freeze lesion model for PMZ as well as with peak expression levels of mGluR5 (Jacobs et al., 1996; Wijetunge et al., 2008).

Western blot analysis has revealed increased expression of mGluR5 protein in freeze lesioned cortex at P16 (Jacobs and Pomictor, unpublished observations). Pyramidal neurons in the PMZ also show an increase in frequencies of inhibitory postsynaptic currents (IPSCs) when the group I mGluR agonist DHPG is applied. LTS cells appear to be selectively altered in this region. AIDA, an mGluR1 selective antagonist, was applied prior to the addition of DHPG and an increase in IPSCs was only seen in microgyric tissue (George and Jacobs unpublished oberservations Intro Fig C). This represents a novel way to activate LTS cells via mGluR5 and could serve as the mechanism for epileptogenic activity. If this is the case mGluR5 antagonists would be an appropriate pharmacological focus for seizure management.

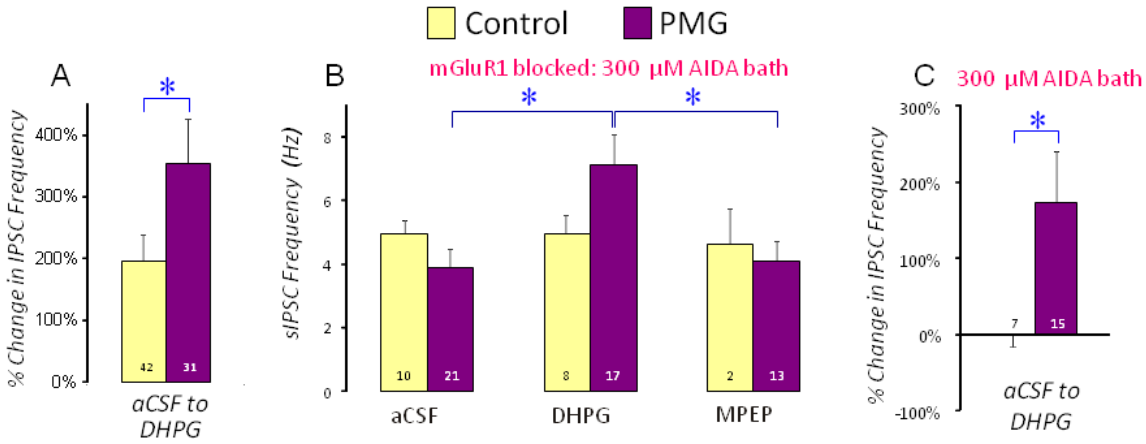

Intro Fig C: The effects of $mGluR_I$ agonists are greater in PMG compared to control cortex. A) In normal aCSF, the addition of the $mGluR_I$ agonist DHPG increases the frequency of IPSCs recorded in layer V pyramidal neurons. This increase is significantly larger in PMG compared to control cortex. B) When mGluR1 receptors are blocked by addition of the selective antagonist AIDA to the bath, there is no change in IPSC frequency with the addition of DHPG in control cortex. In PMG cortex there is still an increase in IPSC frequency that can be blocked by the mGluR5 selective antagonist, MPEP. C) With only mGluR5 receptors active, there is still a large increase in the IPSC frequency, however not as large as when both mGluR1 and mGluR5 receptors are active. Thus in addition to increased expression and/or function of mGluR5 receptors, there is also likely an increase in expression or function of mGluR1 receptors. Numbers in each column indicate the number of pyramidal neurons recorded.

At least three mGluR1 splice variants have been identified: α, β and c (Ferraguti et al., 1998). Antibodies for the β variant has been shown to rarely label cells in cortex while α labels numerous cells (Ferraguti et al., 1998). Less is known of the c variant. Immunoreactivity for

mGluR1α has been previously studied in rat cortex. This study found that all of the mGluR1α immunoreactive cells were also labeled with GABA, however, these cells accounted for only 20% of the total number of GABA expressing cells (Stinehelfer et al., 2000). Labeled mGluR1α cells were seen in all cortical layers with the highest concentration found in layer V (Stinehelfer et al., 2000). Double labeling was performed with markers for PV and SS to distinguish the interneuron subtypes expressing the receptor. The majority of mGluR1α-labeled cells were found to express SS while only one neuron in the entire study co-labeled with PV (Stinehelfer et al., 2000). Fluorescent labeling of oligodendrocyte (OL) cultures have also revealed transient group I mGluR (both 1 and 5) expression in OL precursors, which vanishes in mature OLs (~P10) (Deng et al., 2004). In situ hybridization has been used to verify that no non-neuronal cells express mGluR5 mRNA in adult rat cortex (Mudo et al., 2007). Cortical in situ hybridization labeling has also shown that mGluR1α mRNA signaling is intense in SS positive neurons and not found in PV expressing neurons (Kerner et al., 1997). The hybridization signal for mGluR5 mRNA, however, was significant in both PV and SS expressing neurons (Kerner et al., 1997).

This may help explain the novel mGluR5 activation seen in LTS cells in microgyric cortex. These cells may be capable of producing these receptors, however, may only do so in specific circumstances (such as the reduction of PV) as a compensatory mechanism. In an effort to determine whether this may be occurring fluorescent immunohistochemical stains were performed to co-labeled group I mGluRs with interneuron subtype specific markers to determine which cell types express these receptors and whether they are differentially expressed in PMG cortex.

CHAPTER 2

METHODS

2.1 Freeze Lesion Induction

Aseptic surgery techniques were followed in the induction of the freeze lesion in P1 rat pups. The pups were anesthetized by placing them in an ice bath for four minutes prior to surgery. A rectangular probe (tip size = 2 x 5 mm) was filled with isobutene and placed in dry ice until temperatures of -50 degrees Celsius were reached. An incision was made in the scalps and the probe was placed directly on the skull approximately 2 mm lateral to the midline crossing the bregma and lambda. The probe was held there for five seconds then the skin was sutured and the pup was warmed under a lamp and returned to the dam.

2.2 Transcardial Perfusion

Lesioned pups and their non-lesioned littermates were retrieved on P16-17 and anesthetized with isoflurane. Animals were then perfused transcardially with 0.9% saline followed by 4% paraformaldehyde with picric acid (0.4%). The brains were removed and postfixed in 4% paraformaldehyde with picric acid (0.4%) overnight. The next day, the solution was removed and replaced with phosphate buffered saline (PBS, 0.1M, pH 7.4) for long term storage.

2.3 Slide Preparation

The right hemispheres of the non-lesioned brains were marked to insure correct hemisphere comparisons could be made. Then the brains were sectioned coronally in phosphate buffer (PB, 0.1M, pH 7.4) at a thickness of 40 micrometers using a Leica Vibratome. The hippocampus was used as a cortical landmark in the pairing of lesioned and control cortical sections. At least three different rats were used for each staining combination and up to three sections were used from each rat's brain. Each section was washed three times in PBS for five

minute increments and then washed three times for ten minutes in tris buffered saline (TBS, 0.05M, pH 7.4). The sections were then placed in a multiwall plate filled with 300 microliters of a blocking solution for two hours at room temperature. The blocking solution was 50% normal horse serum, 2.5% Triton X-100 in TBS. Then the sections were washed three times in TBS for 5 minutes each. Sections were then incubated in 300 microliters of a solution containing the primary antibodies overnight on a shaker at four degrees Celsius. The solution was 10% normal horse serum, 2.5% Triton X-100 and the primary antibody concentration varied depending on the specific antibody (Methods Fig 1), in TBS.

The following day each section was washed three times for five minutes each in TBS. Sections were then incubated in a 300 microliter secondary antibody solution for three hours at room temperature covered on a shaker. The secondary antibody solution was comprised of 10% normal horse serum, 0.5% Triton X-100, and secondary antibodies at concentrations that varied depending on which specific primary antibodies they were paired with (Methods Fig 1), in TBS. Each section was then washed three times for five minutes each in TBS, followed by three additional washes for five minutes each in PB. Paired lesion and control sections were then mounted on slides with 0.01 M PB and Prolong Gold anti-fade reagent.

	Antibody Concentrations			
Staining Combination	Primary Antibody	Concentration	Secondary Antibody	Concentration
1	Tocris mGluR5 (Rb) polyclonal IgG (1mg/ml)	1:250	Alexa Fluor 594 goat anti rabbit IgG (H+L) (2mg/ml)	1:500
	Millipore (Ms) GAD67 monoclonal (1mg/ml)	1:250	Alexa Fluor 405 goat anti mouse IgG (H+L) (2 mg/ml)	1:500
	Millipore (Ms) Neuronal Nuclei (NeuN) 488 conjugated antibody (1mg/ml)	1:1000	*none needed	
2	Tocris mGluR5 (Rb) polyclonal IgG (1mg/ml)	1:250	Alexa Fluor 647 goat anti rabbit IgG (H+L) (2mg/ml)	1:500
	Sigma Parvalbumin Clone Parv-19 (Ms) IgG1	1:1000	Alex Flour 568 goat anti mouse IgG (H+L) (2mg/ml)	1:1000
	Peninsula Laboratories VIP (Gp)	1:1000	Vector Labs. Fluorescein anti guinea pig IgG (H+L) (1.5mg/ml)	1:1000
3	Tocris mGluR5 (Rb) polyclonal IgG (1mg/ml)	1:250	Alexa Fluor 594 goat anti rabbit IgG (H+L) (2mg/ml)	1:500
	BD Pharmingen mGluR1α (Ms) monoclonal (0.5mg/ml)	1:1000	Alexa Fluor 488 goat anti mouse igG (H+L) (2mg/ml)	1:1000
4	BD Pharmingen mGluR1α (Ms) monoclonal (0.5mg/ml)	1:1000	Alexa Fluor 647 goat anti mouse igG (H+L) (2mg/ml)	1:1000
	Peninsula Laboratories Somatostatin-14 (Rb) polyclonal	1:1000	Alexa Fluor 568 goat anti rabit igG (H+L) (2mg/ml)	1:1000
	Peninsula Laboratories VIP (Gp)	1:1000	Vector Labs. Fluorescein anti guinea pig IgG (H+L) (1.5mg/ml)	1:1000

Methods Figure 1: The staining combinations (1-4) for slide preparations: including the antibodies used and concentrations.

2.4 Image Capturing and Analysis

To analyze the data in the most efficient way, we chose to use high power images to sample specific regions of cortex. Images were taken at 63x magnification with a Leica TCS-SP2 AOBS microscope. Settings were calibrated using one section for each individual stain. These settings were then universally applied to every section with that stain in control and PMG cortex. Images were taken in five locations: within the microgyrus (or analogous layer II/III in non-lesioned cortex), 1 mm lateral to the microgyrus in layer II/III and in layer V, and 2.5 mm lateral to the microgyrus in layers II/III and V (Methods Fig 2). At each of these locations sequential scan z stacks were captured. Each stack consisted of 12 scans at a 0.28492-micrometer step size, for a total depth examined of 3.4 micrometers. Leica confocal software was then used to average the intensities of these stacks to produce flattened images. Each image was then randomized by an outside individual and renamed. All of the cells within the 238.1 x 238.1 µm frame from the renamed images were then counted using the cell counter available in ImageJ software. Using this software it is possible to count cells on multiple images simultaneously. This was utilized to determine whether overlap occurred between different labels in double or triple labeled sections. After counts were completed the coding for the renamed files was revealed and the data was organized accordingly. Two tailed t tests were then performed for statistical analysis of potential differences between control and malformed cortex.

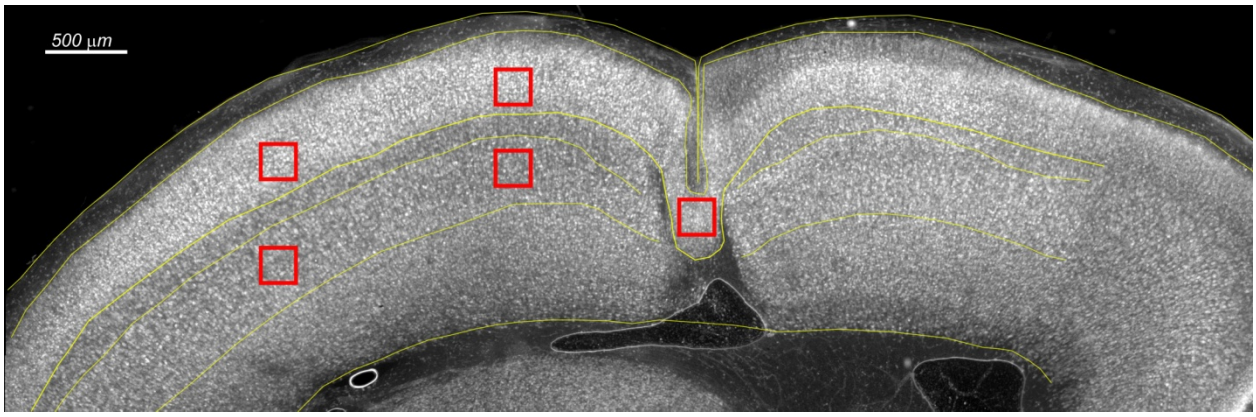

Methods Figure 2: Picture displaying the cortical regions analyzed where high power confocal images were taken from a coronal section through a freeze lesion-induced microgyrus in rat somatosensory cortex. Red boxes represent 238.1 x 238.1 µm frames that were captured with the Leica TCS-SP2 AOBS microscope. All cells within the frame (total depth = 3.4 µm) were counted for each label and every combination of labels.

CHAPTER 3

RESULTS

3.1 mGluR5, GAD67, and NeuN Labeling in Control and PMG Cortex

Triple fluorescent labeling was performed with mGluR5, GAD67 and NeuN antibodies to determine whether there was a difference in the immunoreactivity for these markers in lesioned compared to control cortex (Fig 1). Numerical cell counts in the specified regions yielded no significant differences for each of the individual markers (Fig 2A-C).

Since these markers were used on the same brain sections it was possible to determine generalizations of the overlapping labeled cell populations. 1) It was determined that mGluR5 was found almost entirely in NeuN-labeled cells in both PMG and control cortex (Fig 3D). In the entirety of the study there was only one mGluR5-labeled cell that was not also immunoreactive for NeuN (Fig 3A-C). The one cell observed occurred in the microgyrus of a lesioned animal (Fig 3C). 2) Most of the cells that were immunoreactive for mGluR5 in both control and lesioned cortex were also positive for the GABAergic inhibitory cell marker, GAD67 (Fig 4). In addition, approximately half of the cells that were immunoreactive for GAD67 were also positive for mGluR5 and roughly five percent of the NeuN-labeled cells co-labeled for mGluR5 (Fig 2D, E).

Both statements 1) and 2) are true for malformed cortex. There was, however a significant decrease in the percentage of mGluR5 cells that co-labeled for GAD67, selectively within the microgyrus (Fig 4G), but not within other regions of the PMG cortex. This may reflect an increase in mGluR5 expression in pyramidal and other excitatory neurons within this region, since overall numbers of mGluR5-labeled cells were not different between PMG and control cortex (Fig 2C).

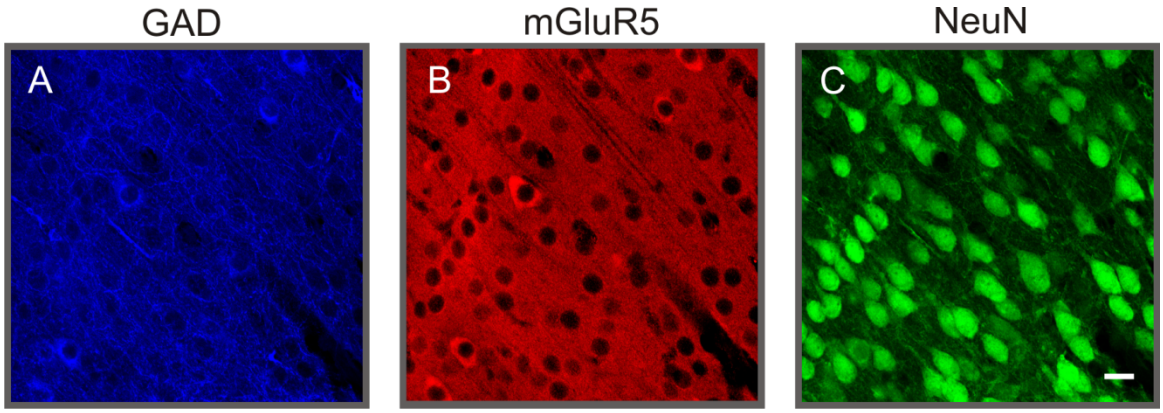

Figure 1: Example of GAD (A) mGluR5 (B) and NeuN (C) immunohistochemical staining. Pictures are of layer III in the region comparable to the PMZ in control cortex.

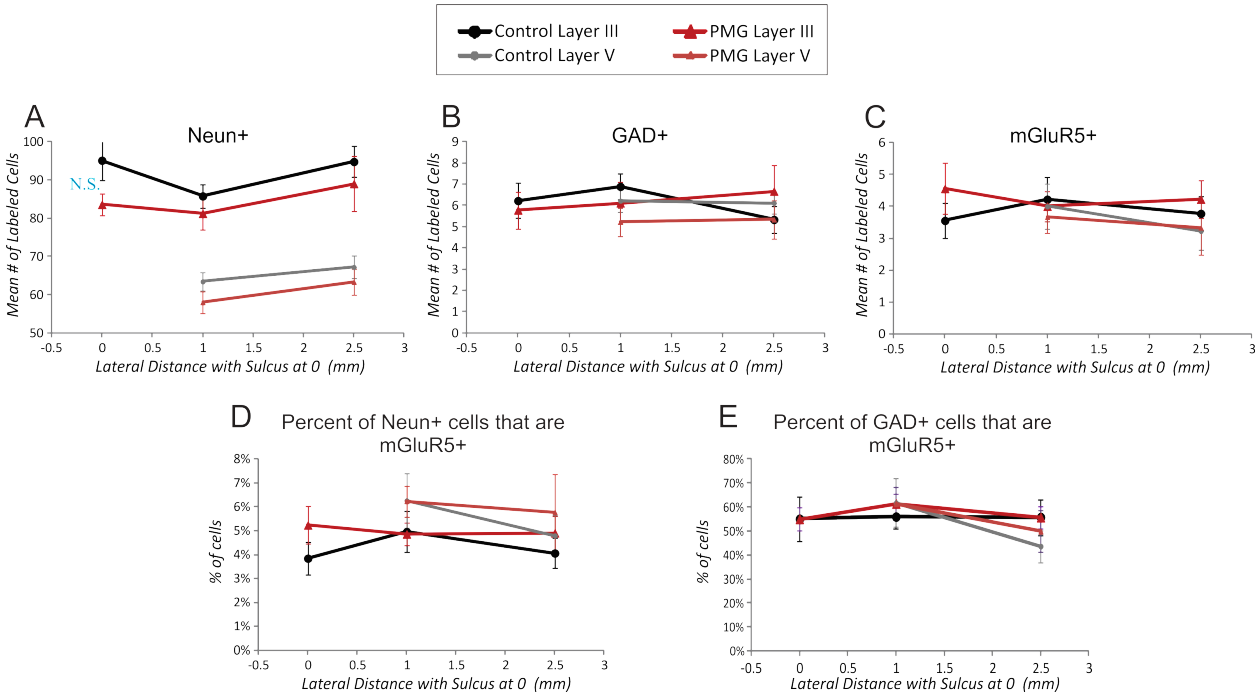

Figure 2: Counts of cells immunohistochemically labeled for Neun (A), GAD67 (B) or mGluR5 (C) and co-labeling results (D,E). There were no significant differences (t-tests, $p>0.05$) between control and PMG in the number of cells that labeled for Neun, GAD, or mGluR5. There was no difference in the percentage of Neun-labeled cells that were mGluR5 positive (D). There was no difference in the percentage of GAD67-labeled cells that were also mGluR5 positive (E).

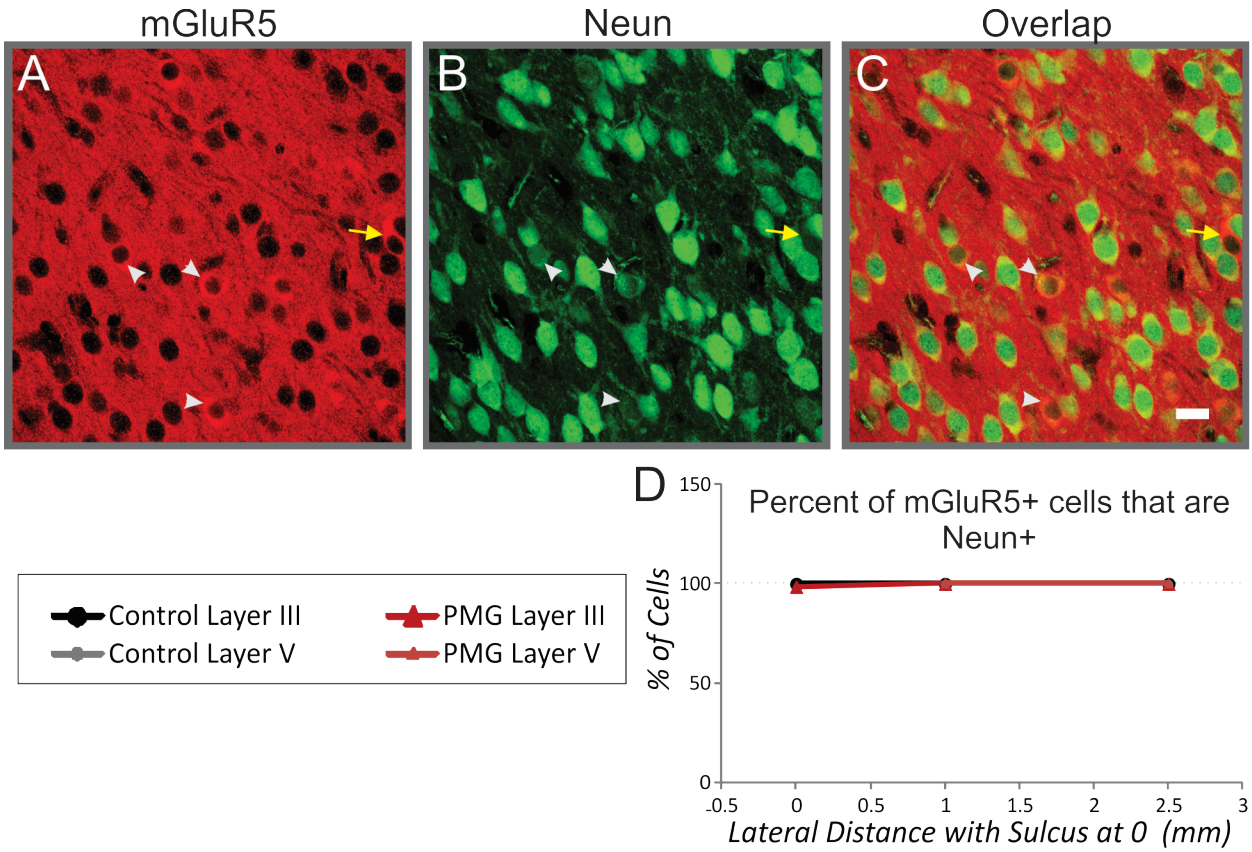

Figure 3: Nearly every mGluR5-labeled cell is also positive for the neuronal marker Neun. Immunohistochemical staining for mGluR5 (A) and Neun (B), with the overlap shown in C. This example is from a PMG section, at a distance 1.0 mm lateral to the microsulcus in layer III. Yellow arrow shows only cell found that did not contain Neun. Gray arrowheads show examples of cells labeled for both mGluR5 and Neun. Scale bar = 20 µm. The percent of mGluR5 positive cells that stained for Neun is shown in D.

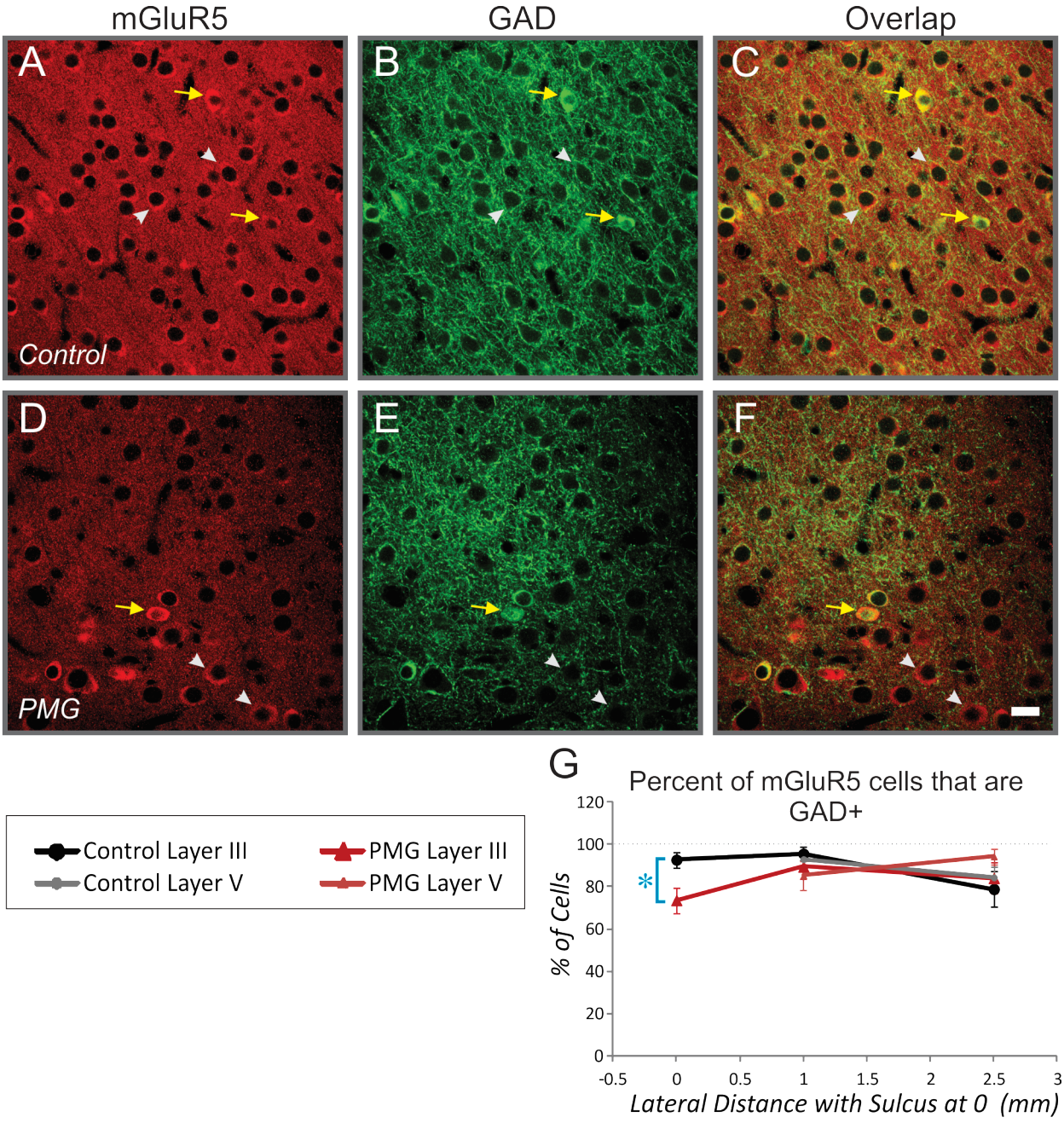

Figure 4: Examples of mGluR5 (A, D) and GAD (B, E) staining in control and malformed cortex. C and F show overlap between the two stains. These pictures are taken within the microgyrus and the comparable region in control cortex. Yellow arrows represent cells that co label for mGluR5 and GAD. White arrows are mGluR5 positive cells that do not label for GAD. G shows that selectively within the microgyrus of malformed cortex there is a decrease in the percentage of mGluR5-labeled cells that are also GAD positive. Scale bar = 20 µm. *= t-test, $p<0.05$.

3.2 mGluR5, Parv and VIP labeling in Control and PMG Cortex

Triple fluorescent labeling was performed with mGluR5 and the two interneuron subpopulation markers: PV and VIP (Fig. 5). Numerical cell counts were made for each of these labels in the specified regions and cortical layers (Fig. 6A, 8A). There were statistically significant differences between the lesioned and control brain sections in these cell populations. There was a significant decrease in PV-labeled cells found in layer V in the region 2.5 mm lateral to the lesion (Fig 6A). This was similar to previous findings; however occurred in a region more lateral (Schwarz et al., 2000). There was also a significant decrease in VIP immunoreactive cells found within the microgyrus of malformed brains (Fig. 8A).

The majority of mGluR5-immunoreactive cells co-labeled for PV (Fig 6B, E and Fig 7). This appeared to be inversely true as most PV-labeled cells were positive for mGluR5 (Fig 6D). There was also overlap seen between VIP and mGluR5 labeling, however, this was very rare (Fig 8B, D, E and Fig 9).

There was a significant reduction in the number of mGluR5 cells that co-labeled for PV in layer V of the region 2.5 mm lateral to the microgyrus in PMG cortex (Fig 6B). However, there was no difference in the percentage of PV cells that were mGluR5 positive (Fig 6D). This suggests that either the observed change has nothing to do with regulation of mGluR5 or that both PV and mGluR5 are collectively down-regulated.

There was an increase in the number of mGluR5-labeled cells that were negative for PV within the microgyrus of malformed cortex (Fig 6C). This was also true for mGluR5 positive cells that were negative for both PV and VIP (Fig 8C). These results indicate that the increase

could either be specific to either mGluR5-labeled SS cells, or pyramidal and other excitatory (non-GABAergic) neurons. However, the increase in mGluR5-positive-GAD67-negative cells within the microgyrus was around 20% of mGluR5 cells (roughly one cell per a frame), while the increase in mGluR5 positive, PV and VIP negative was only around 15% of mGluR5 cells (or roughly 0.5 cells per a frame, Fig 8F). This suggests that the increase is more likely due to non-GABAergic- mGluR5-labeled cells than SS or other GABAergic subtypes.

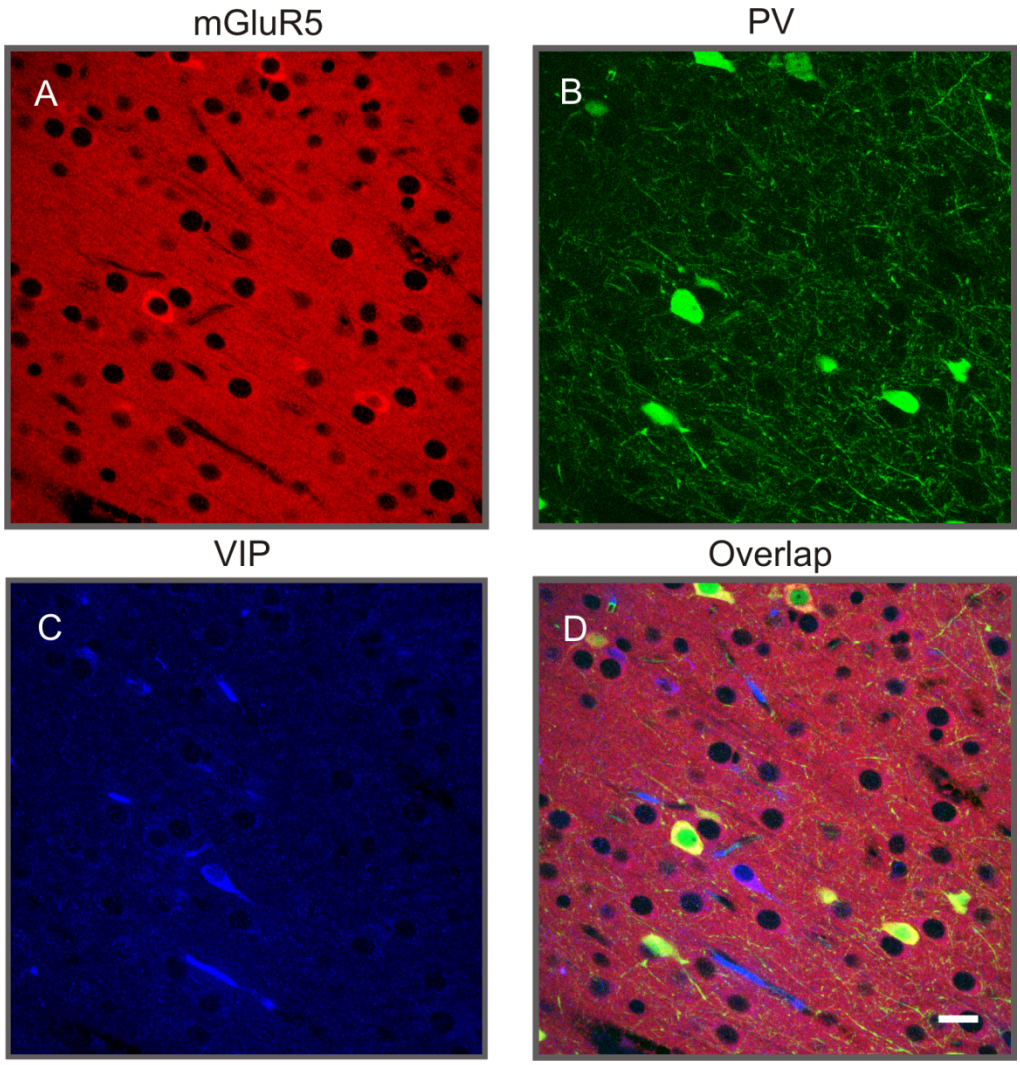

Figure 5: Example of immunohistochemical staining of mGluR5 (A), PV (B), VIP (C) in layer III of the PMZ equivalent region in control cortex. D shows an overlap of all 3 stains. Scale bar = 20 µm.

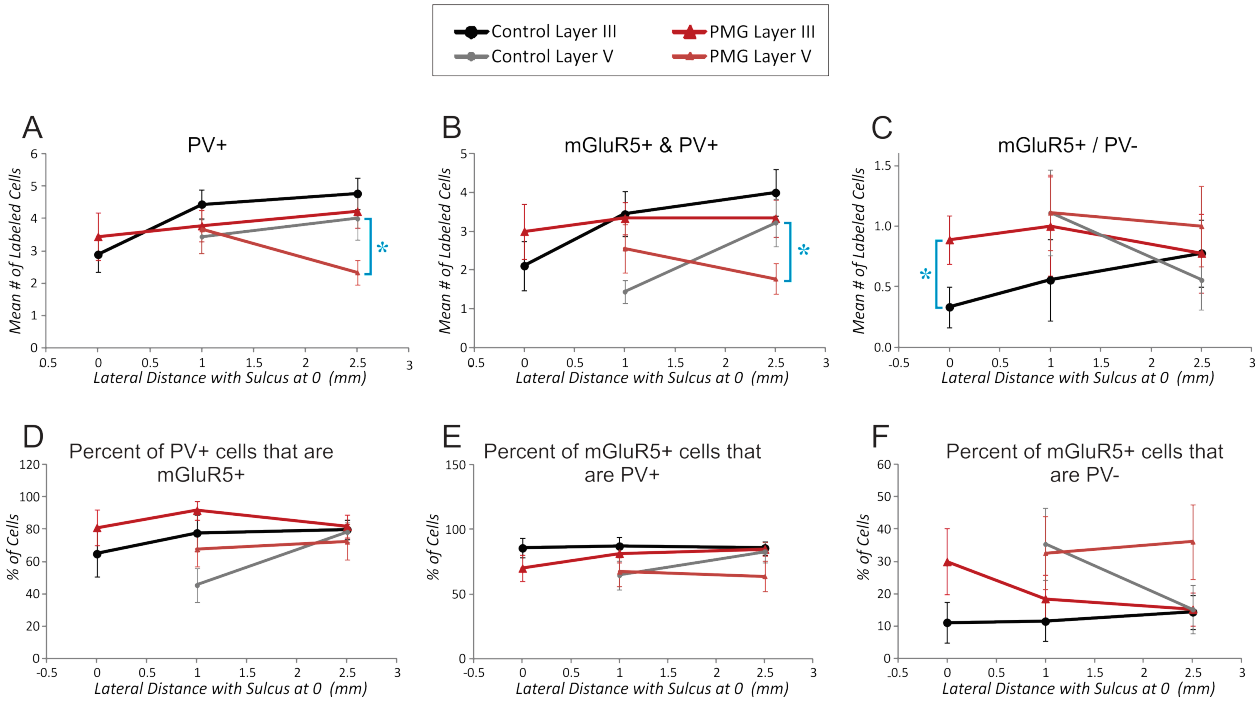

Figure 6: Cell counts and percentage of labeled cells for triple staining with mGluR5, PV, and VIP. There was a selective decrease in PV-labeled cells within the deep layers of the region 2.5 mm lateral to the lesion in PMG compared to control cortex (A). The decrease was also seen in PV cells that were mGluR5 positive (B). There was an increase in the number of mGluR5-labeled cells that were not stained for PV, selectively within the microgyrus of PMG cortex (C). The percentage of PV-labeled cells that were mGluR5 positive was not significantly different between PMG and control cortex (D). The majority of mGluR5 cells co-labeled for PV in both PMG and control cortex (E). There was a trend toward an increase in the percent of mGluR5-positive cells that were not stained for PV in PMG compared to control cortex (F, p=0.07). *= t-test, $p<0.05$.

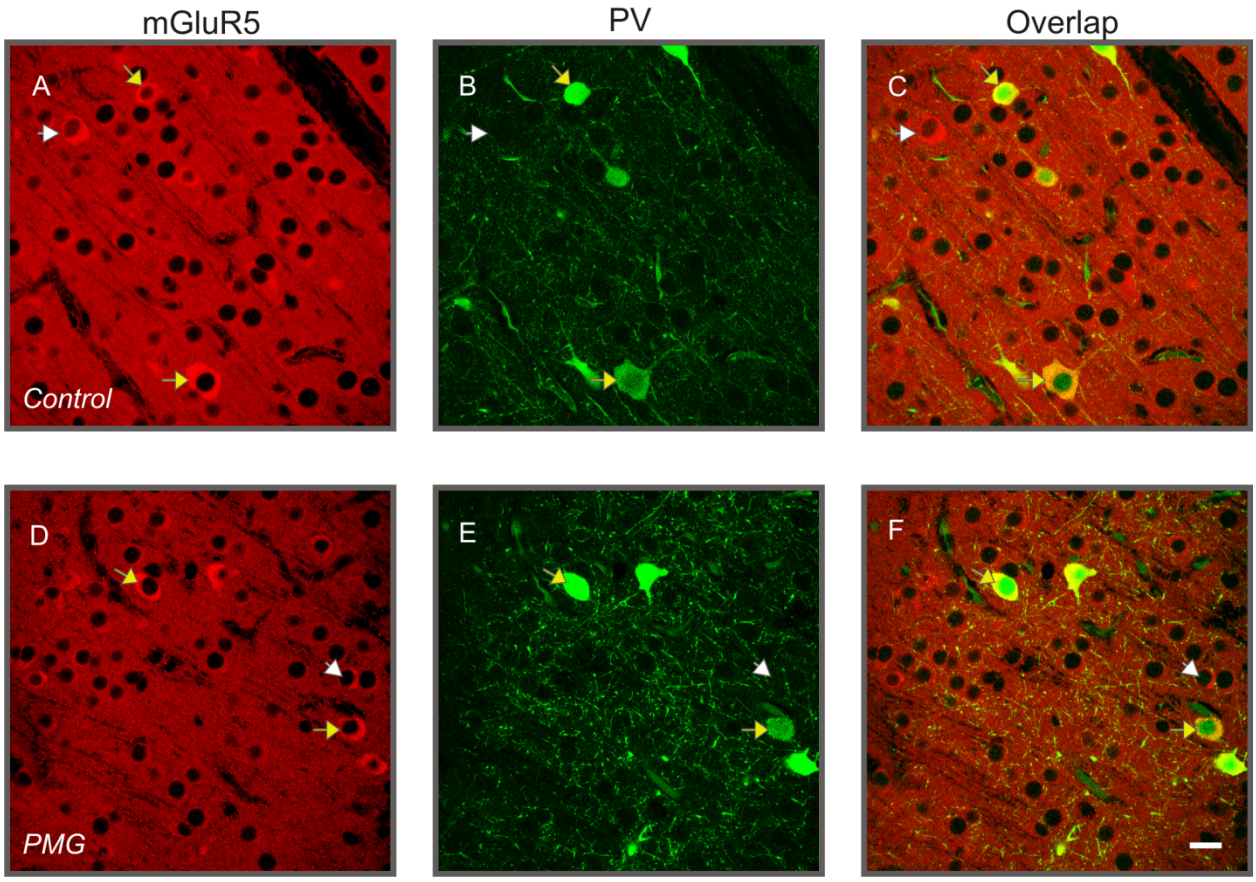

Figure 7: Example of mGluR5 (A, D) and PV (B, E) immunohistochemical labeling for control (A-C) and PMG (D-F) cortex. Yellow arrows are examples of co-labeled cells and white arrows are examples of cells that solely labeled for mGluR5. These pictures were taken in layer III of the PMZ and equivalent region in control cortex. C and F show an overlap of the two stains. Scale bar = 20 µm.

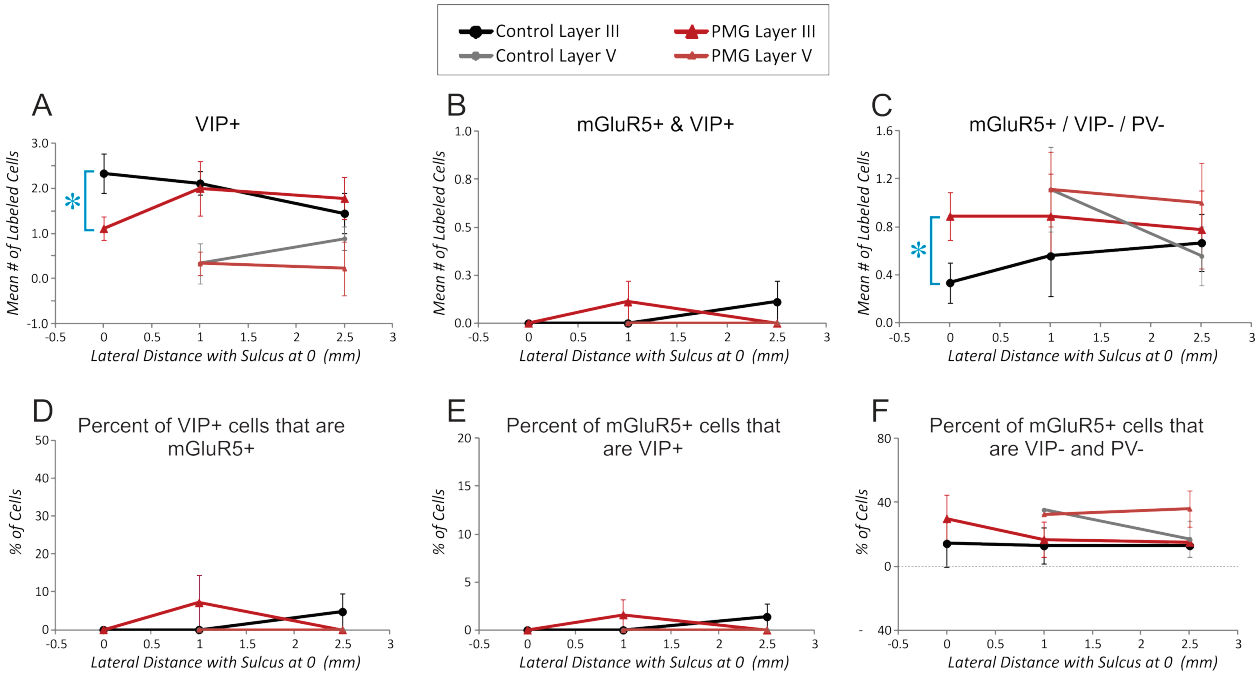

Figure 8: Counts and percentages of cells labeled after mGluR5, PV, and VIP triple staining. There was a selective reduction in VIP-labeled cells within the microgyrus of PMG cortex (A). The mGluR5-labeled cells rarely were VIP positive in either control or PMG cortex (B). There was a selective increase in the number of mGluR5-labeled cells that were negative for both VIP and PV, within the microgyrus of PMG compared to control cortex (C). This may once again reflect an increase in pyramidal or other excitatory neurons that stain for mGluR5 (see Fig 4G). There was no difference seen in the percentage of VIP cells that were positive for mGluR5 (D) or the percentage of mGluR5 cells that were positive for VIP (E). F shows that the percentage of mGluR5-labeled cells that did not label for PV or VIP was not different in control and PMG cortex. *= t-test, $p<0.05$.

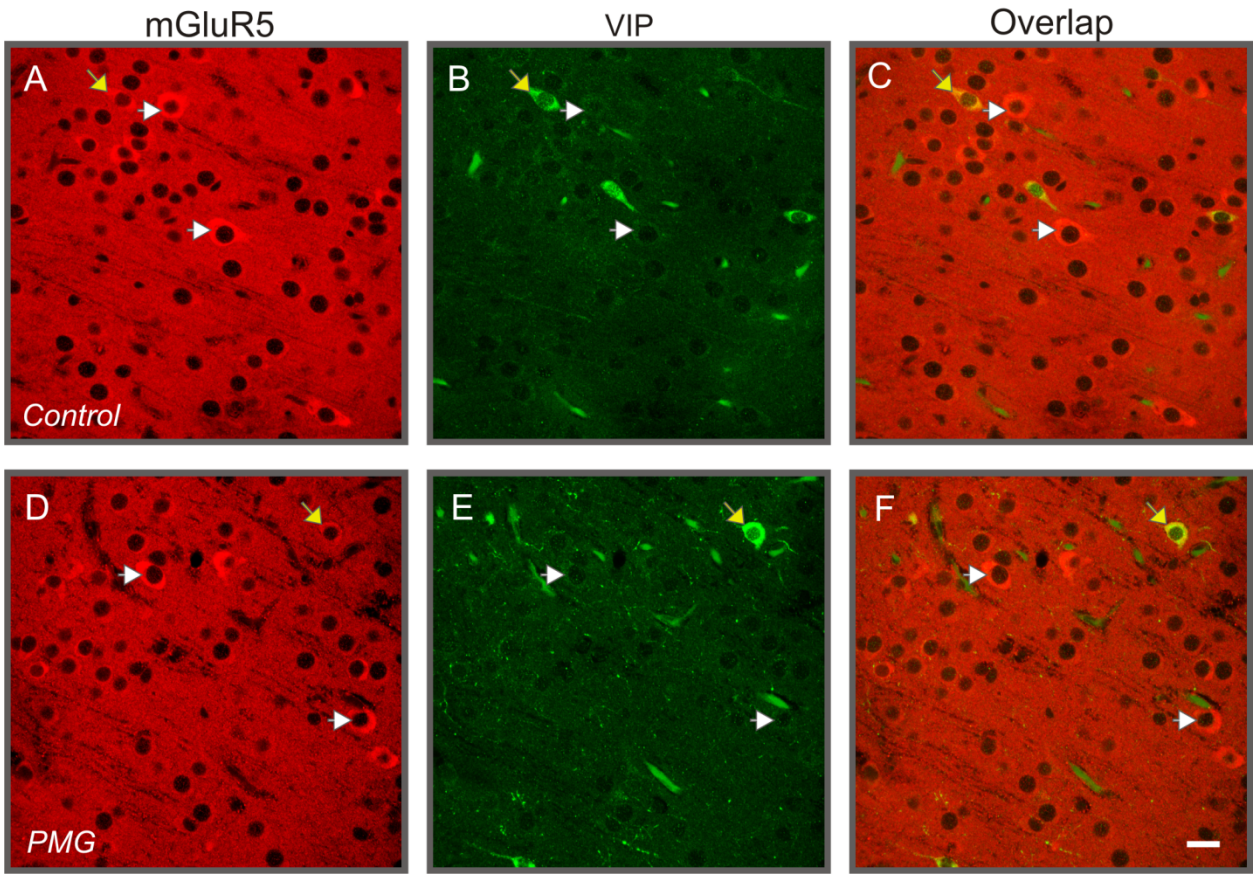

Figure 9: Examples of overlap (C, F) in immunohistochemical labels for mGluR5 (A,D) and VIP (B,E). Yellow arrows are examples of co-labeled cells and white arrows are examples of cells that solely labeled for mGluR5. The co-labeled cell found in control cortex was in layer III 2.5 mm lateral to the region equivalent to the microgyrus in malformed cortex (A-C). The co-labeled cell found in malformed cortex was in layer III of the PMZ (D-F). Scale bar = 20 μm.

3.3 Group I (mGluR1α and mGluR5) Double Labeling in Control and PMG Cortex

Double staining was performed with mGluR5 and mGluR1α markers to determine whether immunoreactive cells for each marker were seen as distinct cell populations (Fig 10). There was a significant decrease in the numbers of cells that stained for mGluR1α within the microgyrus of PMG cortex compared to the equivalent region of control cortex (Fig 11A, t-test,

p<0.05). Labeling in control cortex revealed that there is overlap between group I markers. Around 5-16% of mGluR1α cells were mGluR5 positive while ~13-40% of mGluR5 cells were mGluR1α positive (Fig 11 C, D). There was no difference observed in the numbers of cells that were co-labeled for mGluR1α and mGluR5 in control compared to PMG cortex (Fig 11B-D).

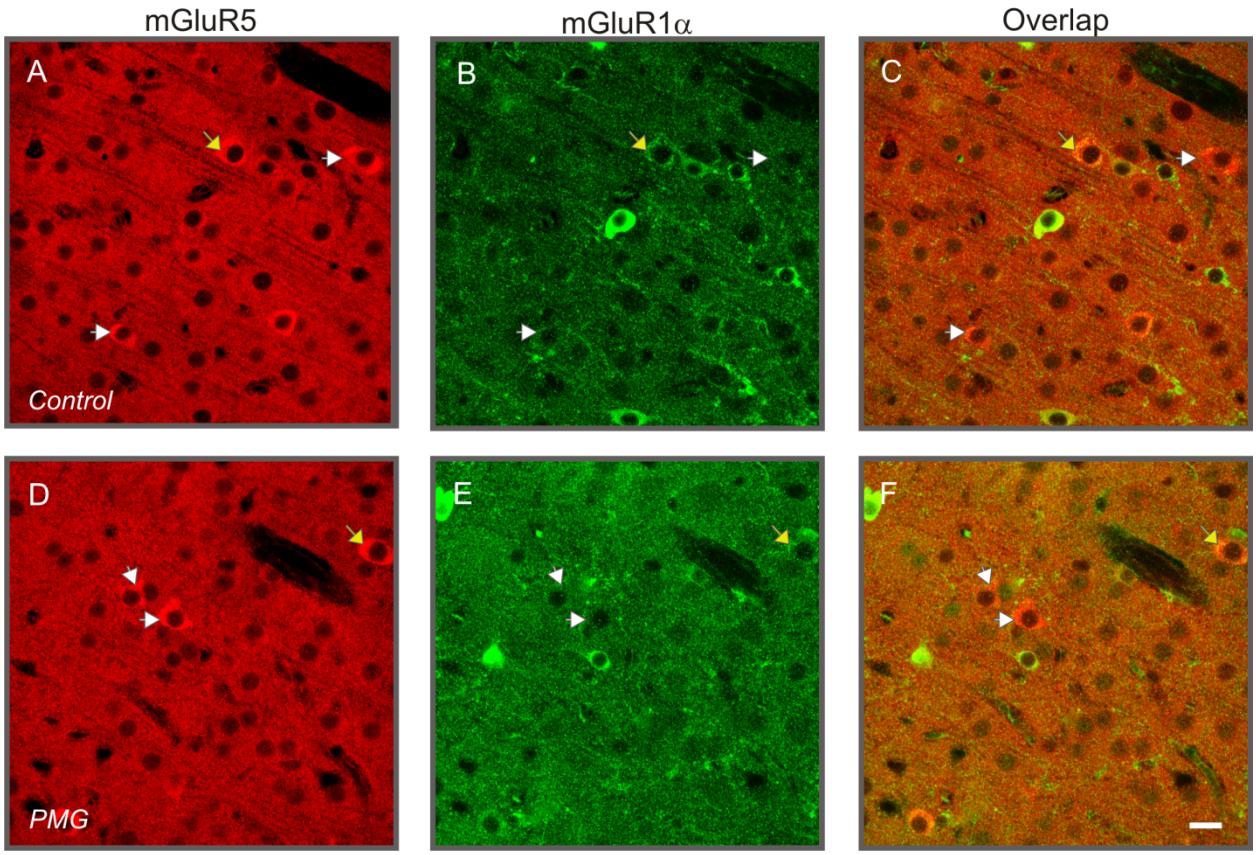

Figure 10: Example of immunohistochemical staining for mGluR5 (A,D) and mGluR1α (B, E) in the same sections of control (A-C) and PMG (D-F) cortex. C and F show overlap with the two stains. Yellow arrows are examples of co-labeled cells and white arrows are examples of cells that solely labeled for mGluR5. Scale bar = 20 μm.

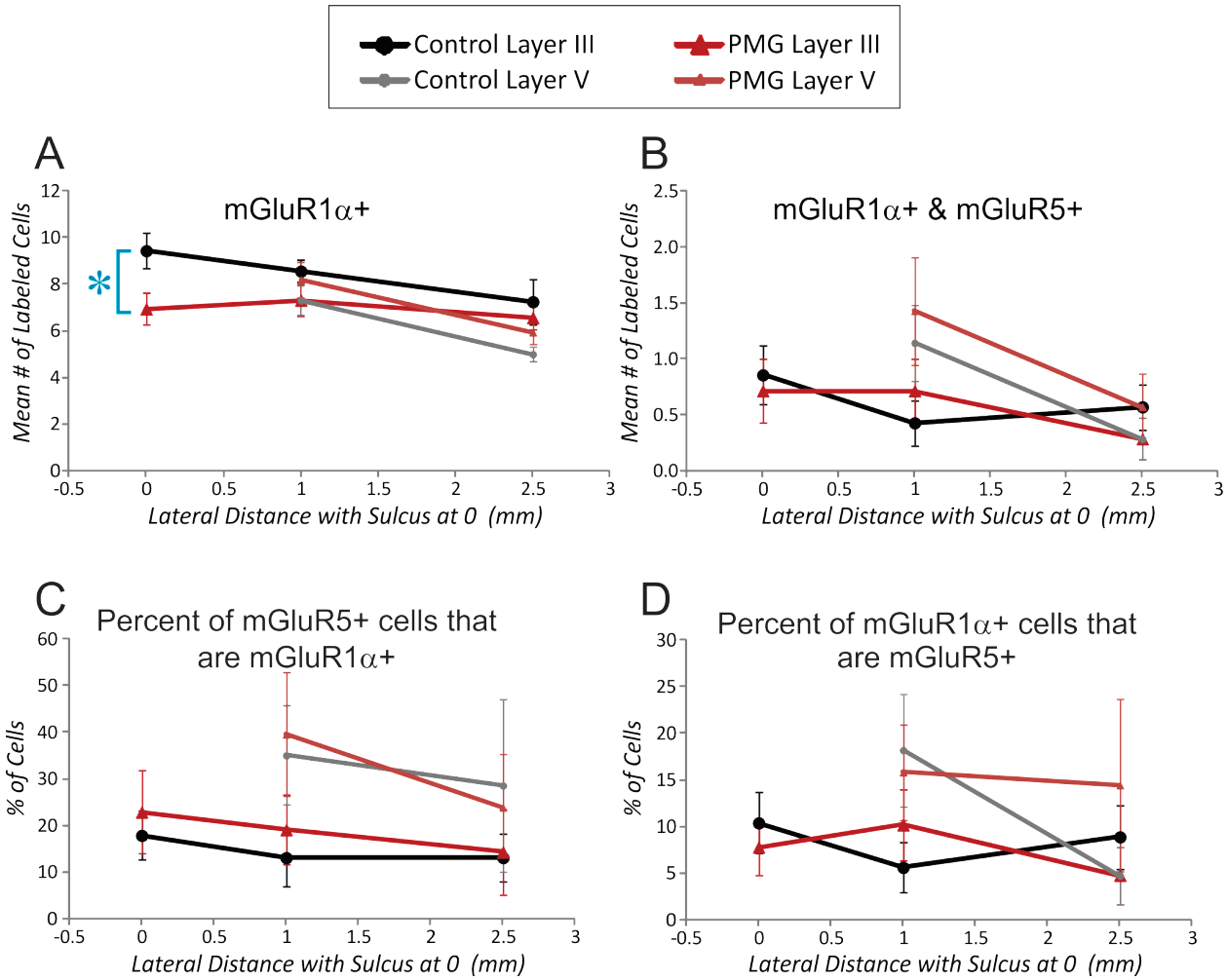

Figure 11: Counts and percentages of cells after double staining for mGluR1α and mGluR5. There was a significant decrease in numbers of mGluR1α-stained cells selectively within the microgyrus of PMG compared to control cortex (A). There were cells that labeled for both mGluR1α and mGluR5; however, no changes were seen in the number of these cells (B). There were also no differences in the percent of mGluR5 positive cells that were mGluR1α positive (C) or the percent of mGluR1α-labeled cells that were mGluR5 positive (D). *= t-test, $p<0.05$.

3.4 mGluR1α, SS and VIP staining in Control and PMG Cortex

Triple fluorescent staining was performed with mGluR1α and the interneuron subpopulation markers: SS and VIP (Fig 12). There were several findings from our control cortex that confirmed previous findings from other labs. Cells that were immunoreactive for mGluR1α overlapped with labeled VIP and SS cells (Figs 13-16). The majority of SS-stained cells were mGluR1α positive (Fig 13D). This was not inversely true as more than half of the mGluR1α-labeled cells were not immunoreactive for SS (Fig 13E). Labeling for mGluR1α was apparent at two intensities. The most intensely mGluR1α-labeled cells were negative for both VIP and SS, however the low-intensity mGluR1α cells often overlapped with these inhibitory interneuron markers (Figs 20, 14, 16). These observations were generally true for both control and PMG cortex.

There was a trend toward an increase in the number of mGluR1α-labeled neurons that were also positive for SS selectively within the microgyrus (Fig 13B, t-test, $p=0.06$) compared to control cortex. This trend was mirrored by a trend toward an increase in the percentage of mGluR1α-labeled cells that were positive for SS (Fig 13E), as well as a significant decrease in the number of cells that were mGluR1α positive but SS negative (Fig 13C). This likely reflects an increased expression of mGluR1α in SS neurons rather than an increase in the number of cells since there was no difference seen in the number of SS neurons within the microgyrus (13A).

The significant decrease in the number of mGluR1α cells that were negative for: SS, VIP or SS and VIP selectively within the microgyrus in malformed cortex (Fig 15C) could represent a loss of expression in PV cells, pyramidal neurons or other cell types (note: NeuN/GAD/mGluR1α staining was not performed due to antibody limitations).

There was a significant increase in the number of mGluR1α positive cells that were negative for VIP in the deep cortical layers at the 2.5 mm location in malformed cortex (Fig 15B). However, this increase was no longer apparent when considered relative to the percentage of mGluR1α immunoreactive cells (not shown, but graph is similar to Fig 15 F). Thus it may be more of a factor of an overall increase in mGluR1α-labeled cells at this location (although when numbers of mGluR1α cells were measured there was no significant difference, see Fig 11A). On the other hand that increase may be selective to cells negative for VIP.

There was a trend towards a reduction in cells that labeled for mGluR1α and VIP in the superficial layers of the PMZ (Fig 15A). Since this trend was also apparent as a trend for percentage of VIP-labeled cells that stain for mGluR1α (Fig 15D), it may reflect a decrease in the expression of mGluR1α in these VIP cells.

After all staining and counting for the results above were completed; observations were made that segregated mGluR1α-labeled cells by the differential level or intensity of staining among cells in both control and PMG cortex. Some mGluR1α cells had a high level of stain (Fig 18). These cells tended to be nearly perfectly round, whereas the lower intensity mGluR1α cells had a more variable shape. The high intensity mGluR1α cells were typically negative for mGluR5 (Fig 19) as well as for VIP and SS labels (Fig 20). The one staining combination that can easily be done but has not yet been performed is mGluR1α with Neun. Thus we do not currently know if the high intensity mGluR1α cells are neurons.

Taking into consideration these apparent distinct populations of mGluR1α-labeled cells, counts were made to determine whether there were differences in their expression in control and malformed cortex. There was a selective increase in the number of high intensity-labeled

mGluR1α cells in layer V of the PMZ (1 mm lateral to sulcus) in malformed compared to control cortex (Fig 17A). These results suggest that there is a selective increase in mGluR1α labeling within an unknown cell type. This same change was seen when calculated as the percent of mGluR1α cells that are high intensity (Fig 17B). This calculation also showed a significant increase in the percent of mGluR1α cells that are high intensity at 1 mm lateral to the sulcus within layers II/III of PMG compared to control cortex. There was a significant reduction in the number of low intensity mGluR1α cells within layers II/III at the 1 mm lateral site of the PMG compared to control cortex (Fig 17C). There may be an increase in mGluR1α expression within the cell populations in the superficial layers and either novel mGluR1α expression in cells in layer V of PMG cortex or an increase in the number of cells that label for mGluR1α at high intensity. The high intensity-labeled mGluR1α cells showed no overlap with SS and rarely overlapped with VIP-labeled cells (3 total cells observed) and mGluR5 (2 total cells observed) (See figures 19 and 20 for typical high intensity mGluR1α cells that show no overlap with these markers).

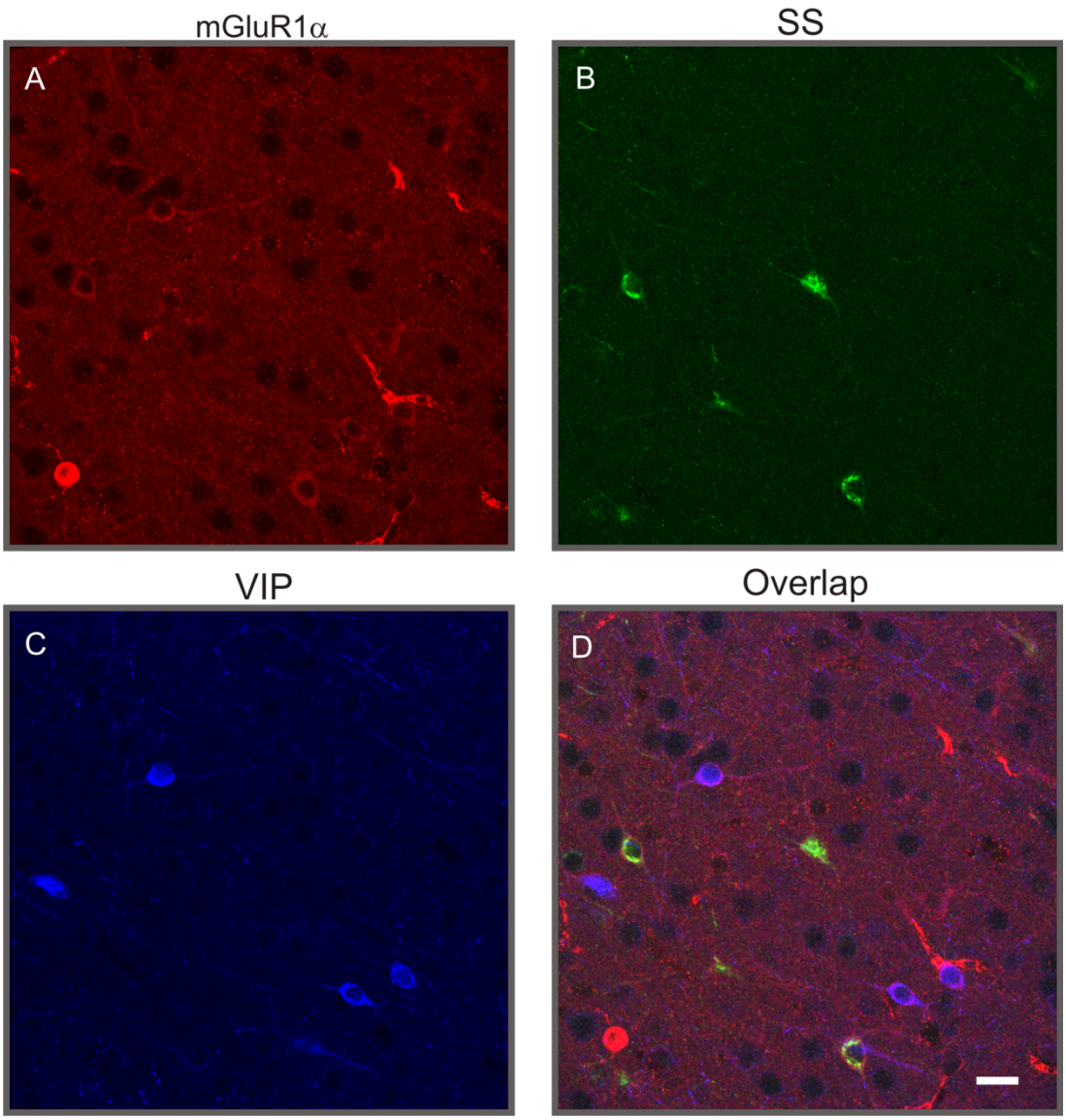

Figure 12: Example of immunohistochemical staining for mGluR1α (A), SS (B) and VIP (C). D is an overlap of the three labels. These pictures were taken in layer III of the region equivalent to the PMZ in control cortex. Scale bar = 20 μm.

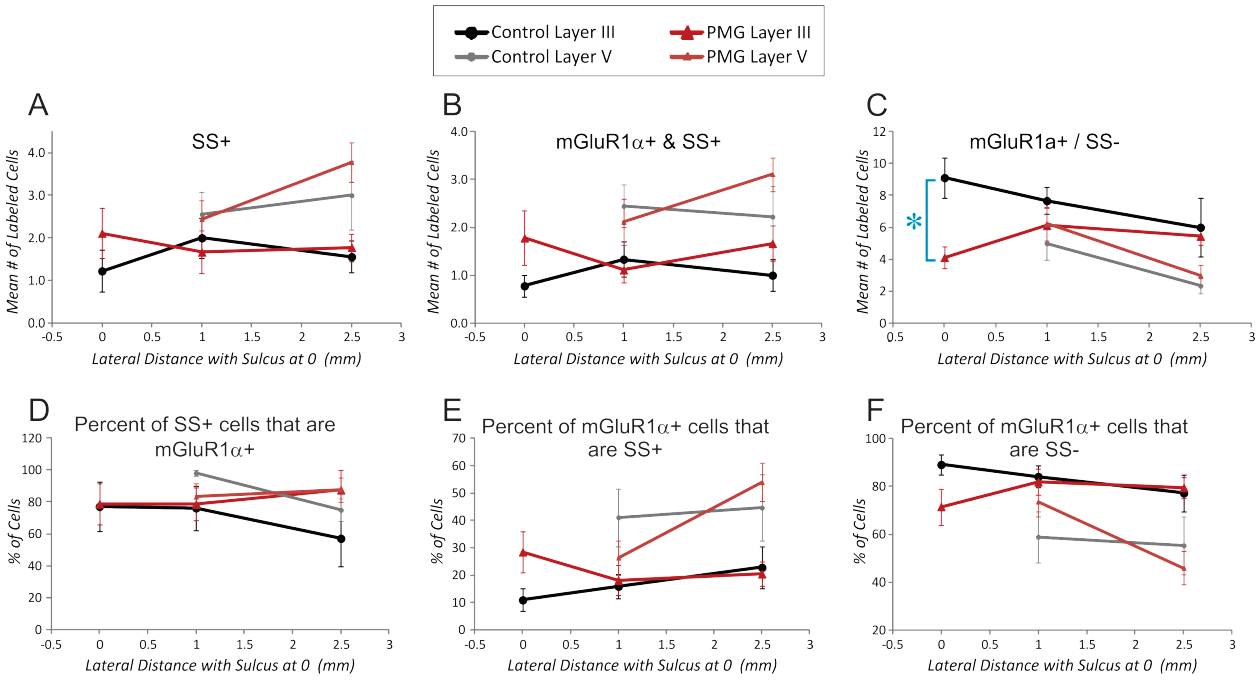

Figure 13: Counts and percentages of labeled neurons after staining for mGluR1α and SS in the same sections. There was no statistical difference in numbers of SS-labeled cells between control and PMG cortex (A). There also was no difference between PMG and control cortex in the number of cells double labeled for mGluR1α and SS, although there was a trend towards an increase within the microgyrus, compared to control cortex (B, t-test, p=0.06). There was a significant decrease in number of mGluR1α positive cells that were negative for SS, selectively within the microgyrus compared to control cortex (C). There was no difference in the percentage of SS-labeled cells that were positive for mGluR1α (D). There was a trend towards an increase in the percent of mGluR1α cells that were also positive for SS within the microgyrus compared to control cortex (E, t-test, p=0.06). That was mirrored by a trend toward a decrease in the percent of mGluR1α cells that were negative for SS, selectively within the microgyrus of PMG compared to control cortex (F, t-test, p=0.06). *= t-test, $p<0.05$.

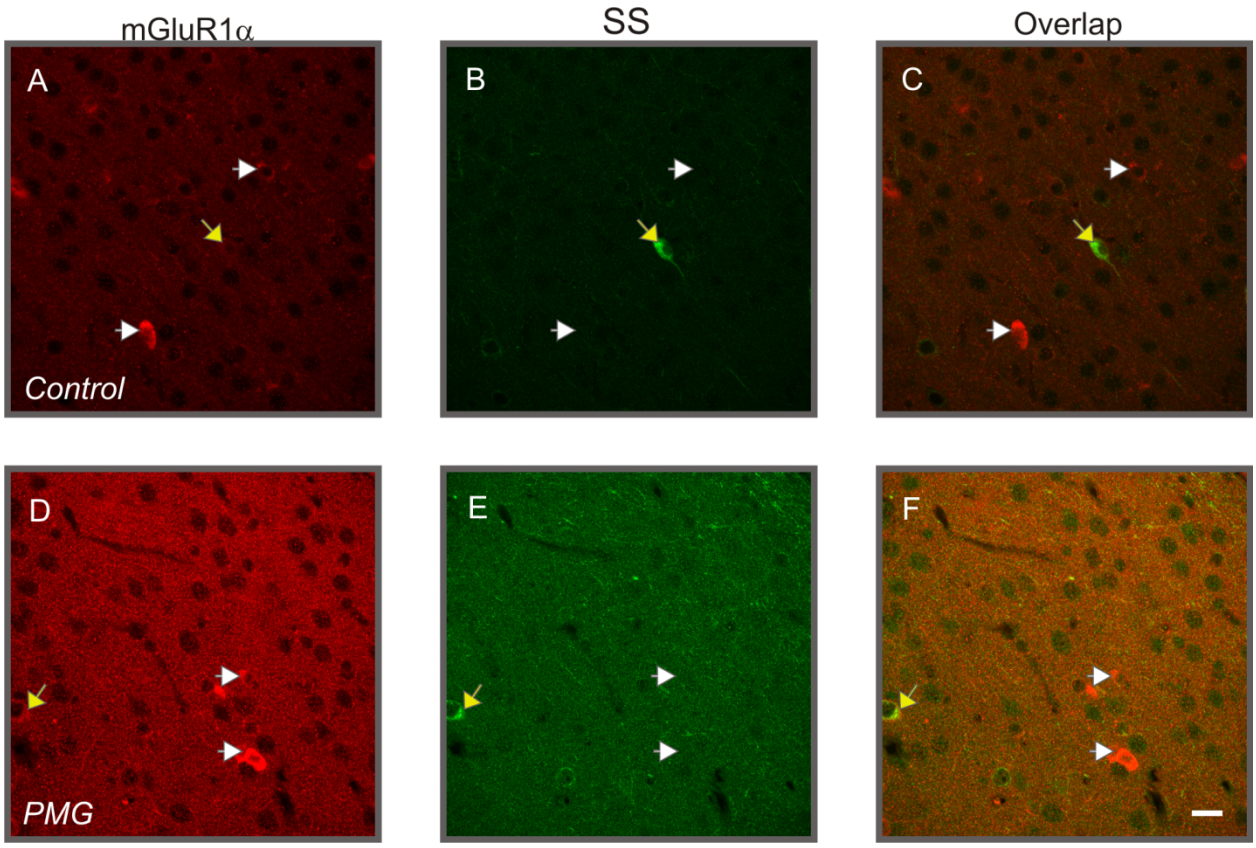

Figure 14: Examples of mGluR1α (A,D), SS (B and E) double immunohistochemical labeling. C and F show overlap of the stains. In the overlap it is apparent that there are cells that are positive for each marker in control (C) and PMG (F) cortex. Yellow arrows are examples of co-labeled cells and white are examples of cells that solely labeled for mGluR1α. Pictures were taken within the microgyrus of malformed cortex and the equivalent region in control cortex. Scale bar = 20 μm.

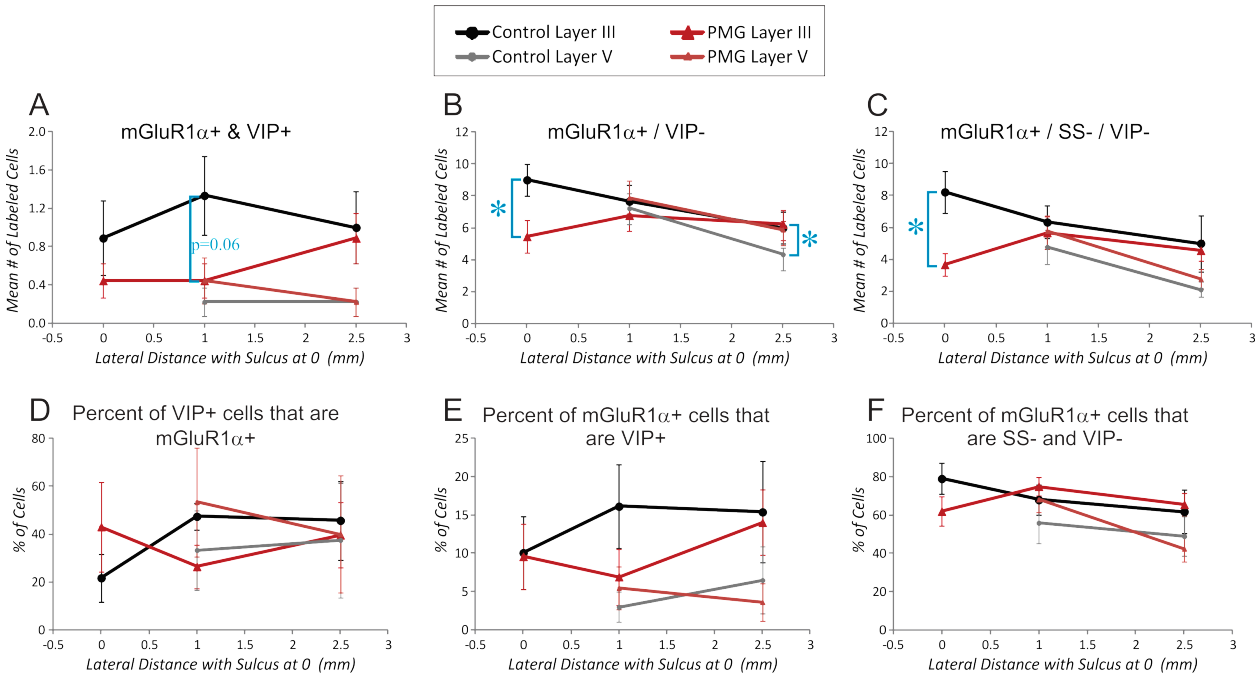

Figure 15: Counts and percentages of labeled neurons after triple staining with mGluR1α, SS and VIP. There was a trend towards a decrease in the number of cells double labeled for mGluR1α and VIP at one millimeter lateral to the sulcus in PMG compared to control cortex (A, t-test, p=0.06). For mGluR1α cells that were not immunopositive for VIP, there was a significant decrease in the microgyrus and a significant increase at 2.5 mm lateral to the sulcus within layer V of PMG compared to control cortex (B). There was also a significant decrease within the microgyrus for mGluR1α cells that were negative for SS and VIP (C). There was no difference between PMG and control cortex in the percent of VIP stained cells that were also positive for mGluR1α (D). There also was no significant difference in the percent of mGluR1α cells that were VIP positive (E), nor in the percent of mGluR1α cells that were both SS and VIP negative (F).

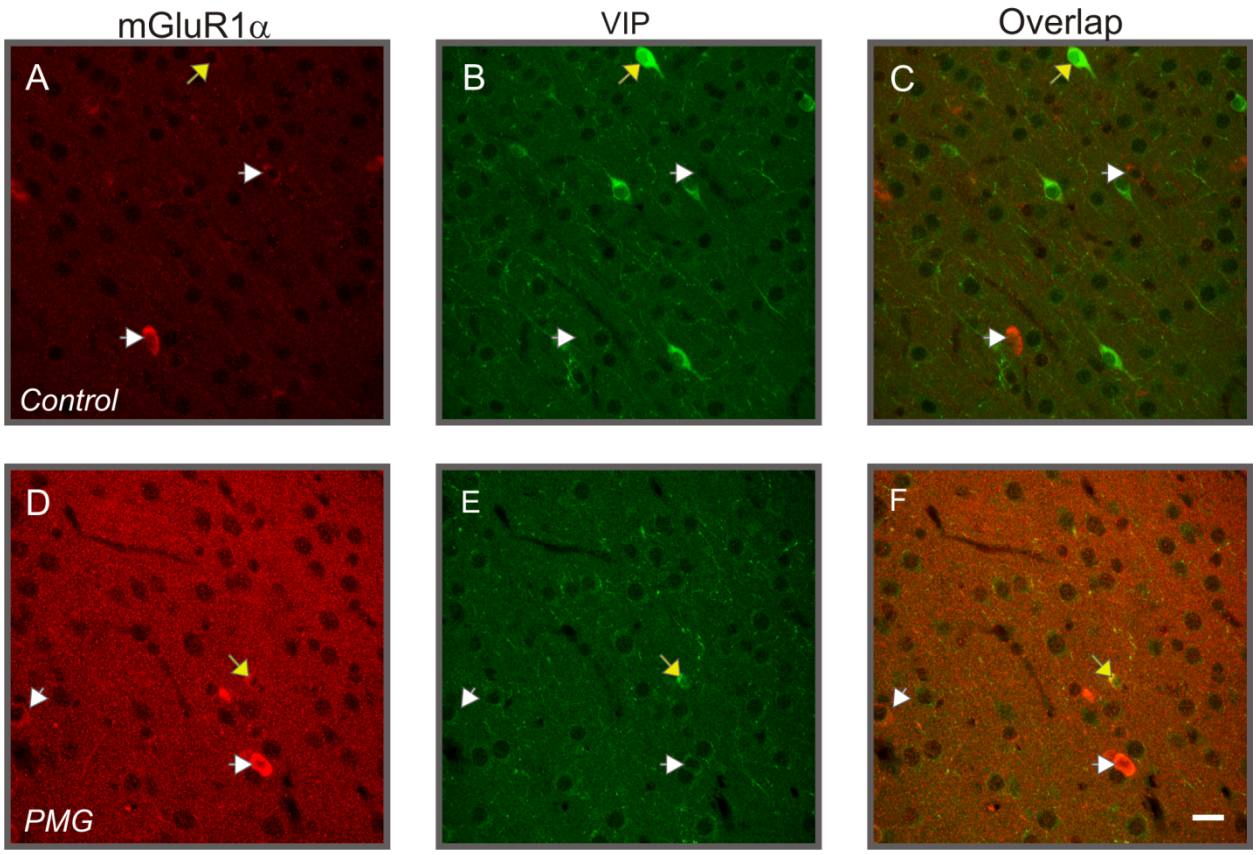

Figure 16: Example of mGluR1α (A, D) and VIP (B, E) double immunohistochemical staining in control and PMG cortex. C and F show there is overlap in labeling of the markers. Yellow arrows are examples of co-labeled cells and white arrows are examples of cells that solely labeled for mGluR1α. These pictures were taken within the microgyrus (Bottom) and equivalent region of control cortex (Top).

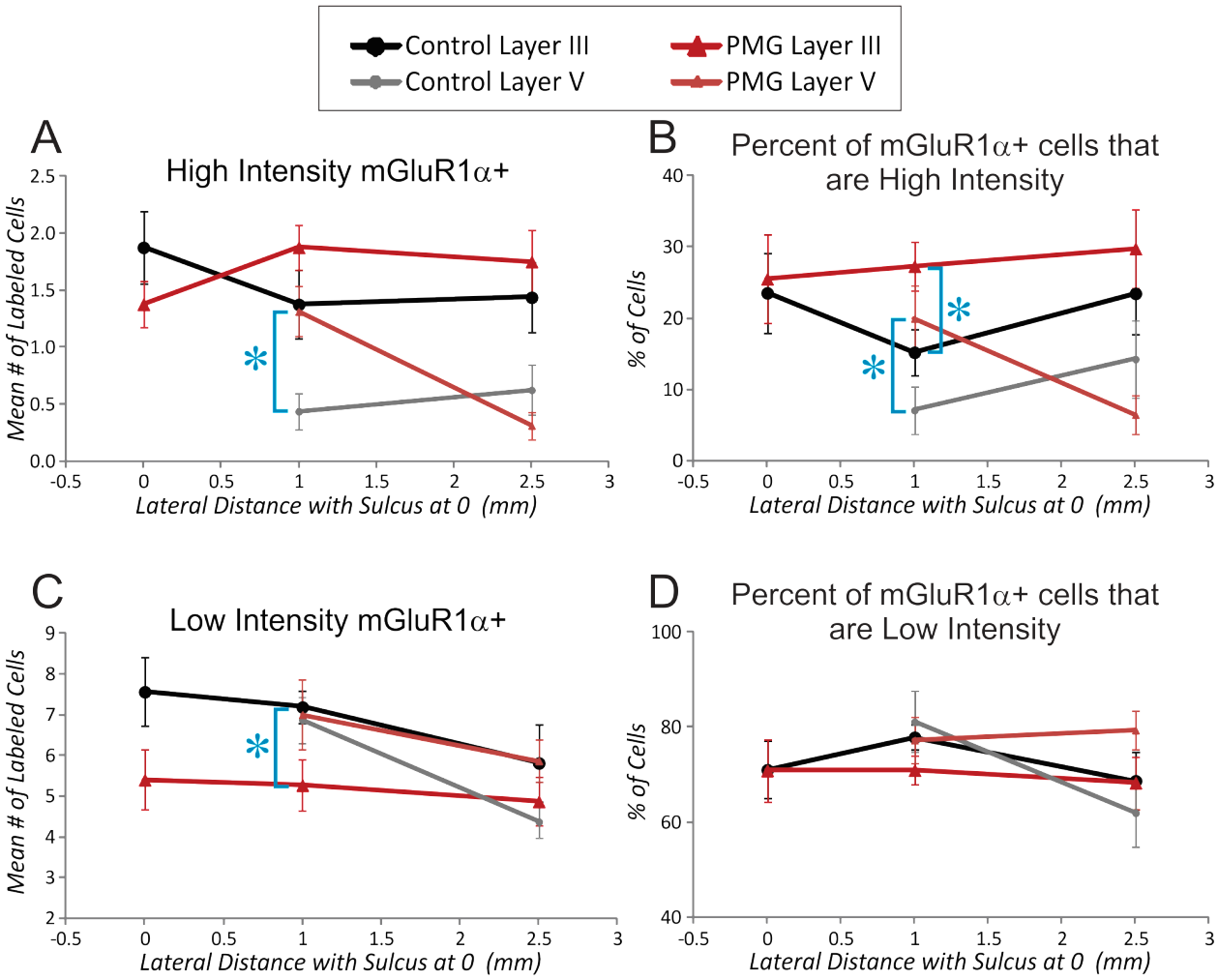

Figure 17: Counts and percentages for high and low intensity labeling of mGluR1α cells. There was a selective increase in the number of high intensity-labeled mGluR1α cells within the deep layers of the PMZ (1 mm lateral to sulcus) in malformed cortex (A). This increase can also be seen in the calculation of the percent of mGluR1α cells that are high intensity-labeled. There is an increase at this location for superficial layers of the PMG compared to control cortex also. There is a selective decrease in the numbers of low intensity mGluR1α cells in superficial layers at the 1 mm site of PMG compared to control cortex (C). When calculated as percentage of mGluR1α cells that are low intensity, there is no significant difference between PMG and control cortex. *=t-test. $P<0.05$.

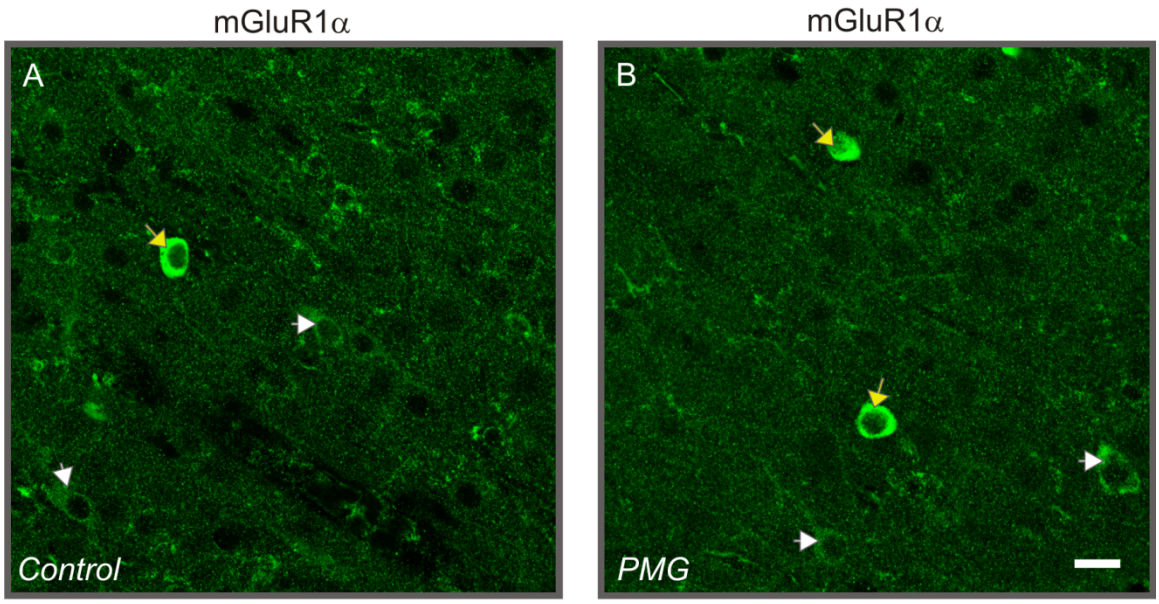

Figure 18: Examples of high intensity (yellow arrows) and low intensity (white arrows) mGluR1α-labeled cells in control (A) and PMG (B) cortex. These pictures were taken in layer III of the PMZ or equivalent region in control cortex. Scale bar = 20 μm.

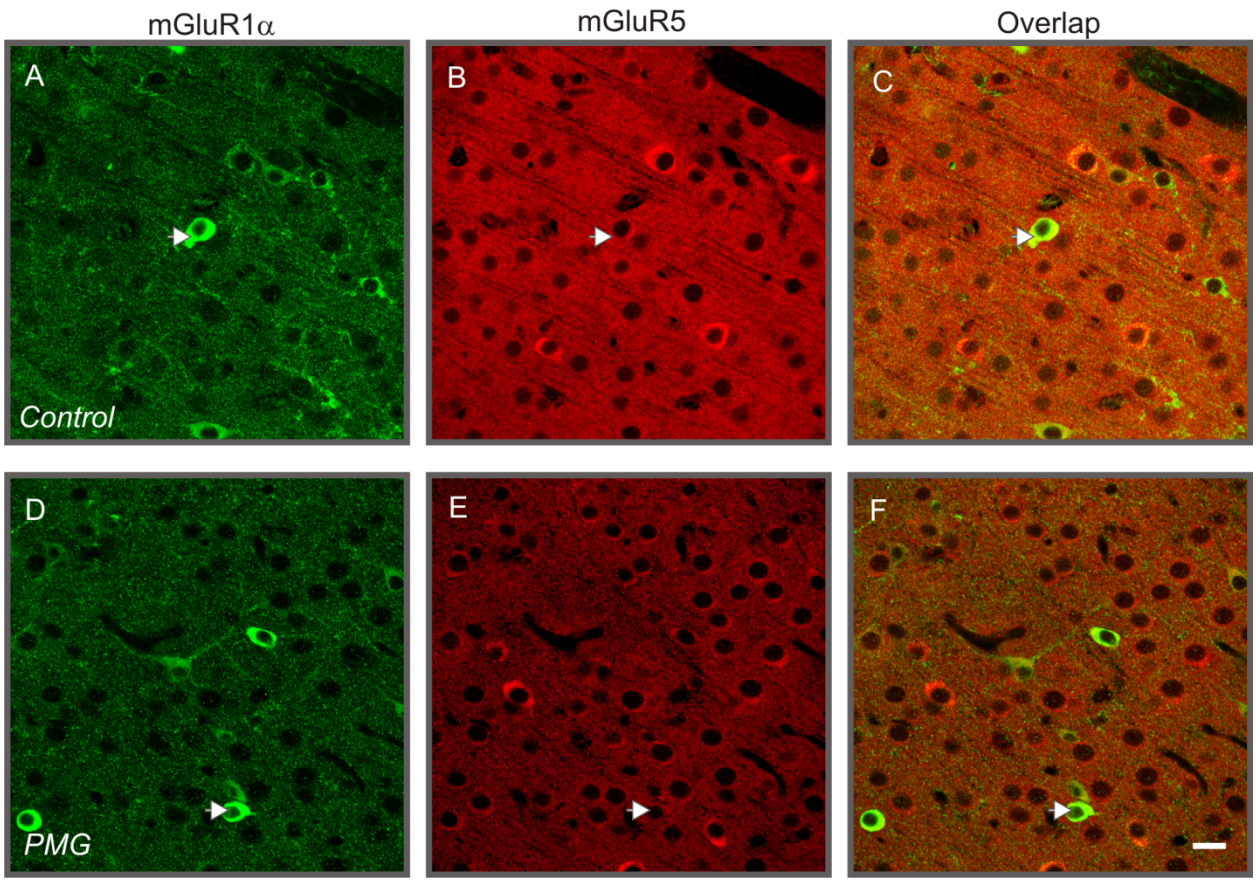

Figure 19: Double immunohistochemical labeling for mGluR1α (A, D) and mGluR5 (B, E) in control (Top) and malformed cortex (Bottom). C and F show overlaps of these markers. High intensity mGluR1α-labeled cells (white arrows) rarely overlap with mGluR5 labeling. These pictures were taken in layer III of the PMZ (Top) and equivalent region in control cortex (Bottom). Scale bar = 20 μm.

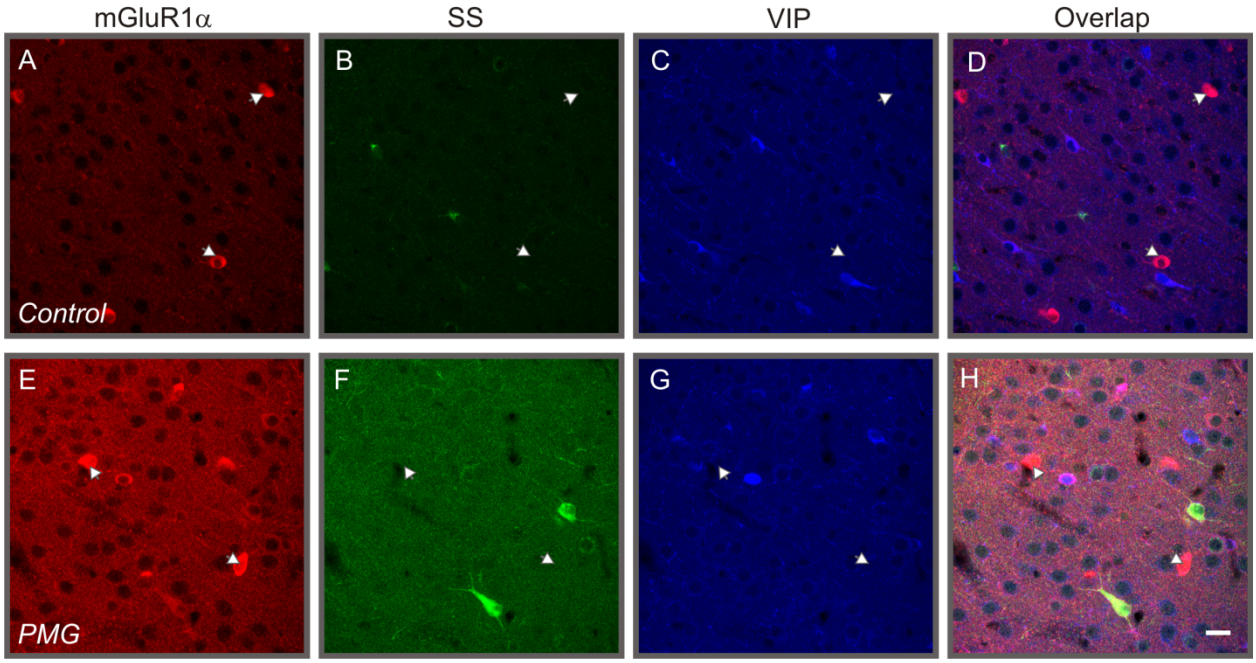

Figure 20: Immunohistochemical labeling for mGluR1α (A, E), SS (B, F), and VIP (C, G) in control (Top) and malformed cortex (Bottom). D and H show overlap. High intensity mGluR1α-labeled cells (white arrows) rarely overlap with SS and VIP positive cells. These pictures were taken in layer III of the PMZ (bottom) and equivalent region in control cortex (Top). Scale bar = 20 µm.

3.5 Results Summary:

The majority of the differences seen in comparing malformed with control cortex appeared to be selective for the region within the microgyrus (Fig 21). There was additionally a selective decrease in the number of PV, and mGluR5/PV co- labeled cells in deep layers 2.5 mm lateral of the microgyrus. There was also an increase in mGluR1α and mGluR1α positive/VIP negative labeled cells within this region. Lastly, there was an increase in the number/percentage of high intensity labeled mGluR1α cells in layer V of the PMZ, and an increase in the percentage of high intensity cells in the superficial layers of the PMZ that coincided with a reduction in low intensity mGluR1α cells.

In PMZ versus control: TD = trend down, ND = no difference, D= significantly decrease, I = Increase, - = too few cells to test					
	MG - LIII	PMZ - LIII	2.5 - LIII	PMZ - LV	2.5 - LV
Series 1					
Neun	TD	ND	ND	ND	ND
GAD	ND	ND	ND	ND	ND
mGluR5	ND	ND	ND	ND	ND
Neun + mGluR5	ND	ND	ND	ND	ND
% of Neun+ that are mGluR5+	ND	ND	ND	ND	ND
% of mGluR5 cells Neun+	ND	ND	ND	ND	ND
GAD + mGluR5	ND	ND	ND	ND	ND
% of GAD+ that are mGluR5+	ND	ND	ND	ND	ND
% of mGluR5 cells GAD+	D	ND	ND	ND	ND
mGluR5+/Neun-	-	-	-	-	-
% of mGluR5+/Neun-	-	-	-	-	-
mGluR5+/GAD-	I	ND	ND	ND	ND
% of mGluR+/GAD-	I	ND	ND	ND	ND
mGluR5+/Neun-/GAD-	-	-	-	-	-
% of mGluR5+ /Neun-/GAD-	-	-	-	-	-
Series 2					
mGluR5	ND	ND	ND	ND	ND
PV	ND	ND	ND	ND	D
VIP	D	ND	ND	ND	ND
mGluR5 + PV	ND	ND	ND	ND	D
% of PV+ that are mGluR5+	ND	ND	ND	ND	ND
% of mGluR5+ that are PV+	ND	ND	ND	ND	ND
mGluR5 + VIP	ND	ND	ND	ND	ND
% of VIP+ that are mGluR5+	-	-	-	-	-
% of mGluR5% that are PV+	-	-	-	-	-
mGluR5+/PV-	I	ND	ND	ND	ND
% of mGluR5+/PV-	ND	ND	ND	ND	ND
mGluR5+/VIP-	ND	ND	ND	ND	ND
% of mGluR5+/VIP-	ND	ND	ND	ND	ND
mGluR5+/PV-/VIP-	I	ND	ND	ND	ND
% of mGluR5+/PV-/VIP-	ND	ND	ND	ND	ND
Series 3					
mGluR1a	ND	ND	ND	ND	ND
mGluR5	ND	ND	ND	ND	ND
mGluR1a + mGluR5	ND	ND	ND	ND	ND
% of mGluR5+ that are mGluR1+	ND	ND	ND	ND	ND
% of mGluR1a+ that are mGluR5+	ND	ND	ND	ND	ND
mGluR1a+/mGluR5-	ND	ND	ND	ND	ND
mGluR1a-/mGluR5+	ND	ND	ND	ND	ND
Series 4					
mGluR1a	D	ND	ND	ND	I
mGluR1a High Intensity	ND	ND	ND	I	ND
SS	ND	ND	ND	ND	ND
VIP	TD	ND	ND	ND	ND
% of mGluR1a that are High Intensity	ND	I	ND	I	ND
mGluR1a + SS	TI	ND	ND	ND	ND
% of SS that are mGluR1a+	ND	ND	ND	ND	ND
% of mGluR1a that are SS+	TI	ND	ND	ND	ND
mGluR1a + VIP	ND	TD	ND	ND	ND
% of VIP that are mGluR1a+	ND	TD	ND	ND	ND
% of mGluR1a that are VIP+	ND	ND	ND	ND	ND
mGluR1a+ / High Intensity-	ND	D	ND	ND	TI
% of mGluR1a+ /High Intensity-	ND	ND	ND	ND	TI
mGluR1a+/SS-	D	ND	ND	ND	ND
% mGluR1a+/SS-	TD	ND	ND	ND	ND
mGluR1a+/VIP-	D	ND	ND	ND	I
% mGluR1a+/VIP-	ND	ND	ND	ND	ND
mGluR1a+/SS-/VIP-	D	ND	ND	ND	ND

Figure 21: Overall summary of all cell counts performed. Cells marked I are significant increases. Those marked D is significant decreases. TI and TD are trend increase and trend decrease respectively. Cells marked ND were those in which no difference was seen and – indicates too few cells were counted to test.

3.6 Additional Statistical Tests:

A two-way ANOVA (group versus location) with repeated measure (3 slides from which measurements were taken) was performed as an additional statistical measure. The groups were control and PMG. The five locations were MG (the microgyrus), layers III and V at 1.0 mm lateral to the MG, layers III and V at 2.5 mm later to the MG. This analysis showed a significant interaction between group and location for the high intensity mGluR1a labeled cells. Pairwise contrasts showed that for this marker, layer V of the PMZ region of PMG cortex was significantly increased compared to the homologous region of control cortex. There were no other significant differences in group or the interaction between group and location. A number of stains showed significance in location, which in most cases was due to a difference between layer III and layer V. Since some group and interactions were near significance (ex. $p=0.07$), likely additional animals should be included in this study.

CHAPTER 4

DISCUSSION

4.1 Discussion

The aim of the present study was to determine whether there were alterations in group I mGluR expression in interneuron populations in freeze lesion induced malformed cortex. Immunohistochemical labels used were: NeuN, GAD67, PV, SS, VIP, mGluR1α and mGluR5. The following observations were made in both control and malformed cortex: (1) mGluR5 labeling is seen almost entirely in neurons; (2) the majority of mGluR5 positive cells were GAD-labeled interneurons; (3) The majority of mGluR5 and mGluR1α labeling does not overlap; (4) mGluR1α labeling occurs at two intensities (high and low), with the high intensity-labeled cells not staining for mGluR5, SS or VIP.

Several previous studies have reported alterations in specific interneuron populations in malformed cortex (Jacobs et al., 1996; Rosen et al., 1998; Schwarz et al., 2000). Our findings corroborate a decrease in PV staining in the deep layers lateral to the microgyrus, which has been shown to persist in older animals (Rosen et al., 1998). This finding is significant considering withdrawal of inhibition is thought to be a mechanism for epilepsy (Dichter and Ayala, 1987). However it is not currently known definitively whether or not the loss of PV-labeled cells actually reflects a loss of inhibitory neurons. In fact, our findings support the idea that there is not a loss in the total number of GAD-labeled cells in malformed cortex (Schwarz et al., 2000). We did, however, see a selective reduction in VIP-labeled cells within the microgyrus of PMG cortex. This has not been previously reported in the freeze lesion model. Interestingly, there was not a reduction in the number of GAD-labeled cells in this region, nor was there an increase seen in the number of SS or PV-labeled cells. This implies that either a portion of GAD-labeled cells lost their immunoreactivity to the VIP antibody, or there may be slight indistinguishable increases in the number of SS- and PV-labeled cells to compensate for the reduction.

There were no dramatic changes observed in numbers of group I mGluR-labeled cells that were co-labeled with the specific interneuron markers used here, except selectively within the microgyrus. These alterations may contribute to the hyperexcitable state of the cortex, although the epileptiform activity is thought to originate from the adjacent PMZ rather than the microgyrus itself. There was a selective decrease in the number of mGluR1α-labeled cells within the microgyrus of malformed cortex. This reduction could be explained by previous findings that mGluR1α plays a role in neonatal hypoxia/ischemia excitotoxicity (Xu et al., 2007; Zhou et al., 2009). This excitotoxicity was seen to occur by means of glutamate release in cortical cultured neurons (Xu et al., 2007). This release acts on NMDA receptors which cause calpain-mediated truncation of the C terminal domain of mGluR1α receptors(Xu et al., 2007). This truncation does not result in a loss of function in the receptor; instead alters the intracellular signaling (Xu et al., 2007). This ultimately leads to a reduction in the phosphorylation of downstream proteins (Akt) and, ultimately, in increased cell death (Xu et al., 2007). The inhibition of this truncation by means of a fusion peptide was shown to have neuroprotective effects (Xu et al., 2007). The truncation of mGluR1α also results in a translocation of the receptors from the dendrites to axons (Xu et al., 2007). No change was observed in the levels of mGluR5 indicating it is not truncated in a similar fashion (Xu et al., 2007).

Interestingly Group I mGluRs have also been shown to have neuroprotective properties (Baskys et al., 2005). Long term treatment with DHPG, prior to administered NMDA, reduced excitotoxic injury in hippocampus cultured neurons (Baskys et al., 2005). The therapeutic implications of these studies for patients with PMG are limited considering the application of mGluR1α antagonists to prevent hypoxia/ischemia excitotoxicity would have to be administered

not only during pregnancy but prior to diagnosis and even prior to the event that creates the malformation. This does not seem feasible.

The neuroprotective properties of group I mGluRs may, however, explain the selective reductions seen in specific cell populations. There was a reduction seen in mGluR1α-labeled cells within the microgyrus; however, there was no reduction in cells that co-labeled for mGluR1α and mGluR5. These cells may have remained active prior to and during the hypoxic event and thus were protected. There was also a trend seen towards a selective increase in mGluR1α-labeled cells that were SS positive within the microgyrus of PMG cortex. This trend was mirrored by an increase in the percentage of mGluR1α-labeled cells that were positive for SS. If true, this likely represents an increase in the expression of mGluR1α in SS neurons rather than an increase in the number of cells since there was no increase observed in SS-labeled cells within the microgyrus. There was also a selective decrease within the microgyrus in the number of mGluR1α-labeled cells that were either negative for SS or VIP, or were negative for both markers. This may reflect a loss, or reduction, of mGluR1α expression within PV, pyramidal neurons or glial cells.

There was a decrease seen in the percentage of mGluR5-labeled cells that were GAD-positive selectively within the microgyrus in PMG cortex. There was no difference seen in the number of mGluR5, and GAD-labeled cells in control and lesioned animals. This suggests that there is an increased expression of mGluR5 in pyramidal or other non-GABAergic neurons within this region. Additionally, in sections triple-stained for mGluR5, VIP and PV showed a selective increase, within the microgyrus, of mGluR5-labeled cells that were *negative* for PV or negative for both PV and VIP. This could reflect increased expression in SS interneurons or in pyramidal and other non-GABAergic neurons. There was a reduction in the number of mGluR5-

labeled PV positive cells in the microgyrus, however this reduction lost significance when viewed as the percentage of PV cells that were mGluR5 positive. This suggests that the change observed may have nothing to do with the regulation of mGluR5 or both PV and mGluR5 may be down-regulated together.

These selective alterations within the microgyrus may have significant effects in neuronal networks; however, it has previously been shown that resection of the microgyrus has no effect on the generation of epileptic activity in the PMZ (Jacobs et al., 1999a). Also, similarly, it has been shown that stimulation within the microgyrus does not generate the late multiphasic epileptiform activity seen in the PMZ (Jacobs et al., 1999a).

There was an increase in the number of mGluR1α-labeled cells that were negative for VIP at the distance 2.5 mm lateral to the microgyrus within the deep layers, relative to the homologous region of control cortex. This increase was not apparent when considered relative to the percent of all mGluR1α-labeled cells. Thus the increase may be due to an overall increase in mGluR1α staining or the increase may be selective to VIP negative cells. There was a trend towards a selective decrease in mGluR1α-labeled cells that were positive for VIP in the superficial layers of the PMZ. This was also seen in the percentage of VIP cells that were mGluR1α-positive and thus may reflect a decrease in the expression of mGluR1α in VIP cells. These alterations in regions distant to the microgyrus reflect the vast extent of the abnormalities associated with this malformation.

Previous physiological findings suggest a novel mechanism for the activation of LTS cells via mGluR5 within the PMZ of malformed cortex. In conducting this experiment it was hypothesized that a difference would be apparent in mGluR5 labeling within interneurons in the

PMZ. This difference was not observed, as there was no large increase seen in cellular expression that could account for the significant change in the mGluR5 physiology. However, this does not rule out altered expression of the receptor within interneuron subtypes. One possible explanation is an increase in receptor expression at the membrane level in mGluR5-labeled cells. One method that could be used in future studies for determining whether this was occurring would be through electron microscopic receptor localization (Lujan, 2004). This method can be used to determine the location and density of G protein coupled receptors (Lujan, 2004). Specifically the postembedding immunogold technique is used to localize synaptic receptors (Lujan, 2004). Another potential explanation for the mGluR5 physiology is an increase in the efficacy of the individual postsynaptic receptors. One method to analyze the levels of response would be to use calcium imaging to measure the intensity of calcium signaling in cells (Gobel and Helmchen, 2007).

As previously mentioned, mGluR1α-labeling occurred at two intensities. When analyzed separately, high intensity mGluR1α cells show nearly zero overlap with VIP, SS and mGluR5 labeling. There is a selective increase in the number and percentage of high intensity mGluR1α-labeled cells in layer V and in the percentage of high intensity cells in layer III of the PMZ.

The increase in high intensity mGluR1α-labeled cells may account for the increased physiological response in the deep layers of the PMZ to group I mGluR agonists. It does not, however, address the dramatic change in the mGluR5 physiology. Follow-up studies are necessary to determine the subtype of these high intensity mGluR1 α-labeled cells: interneuron, pyramidal or glial. These cells are seen in both control and malformed cortex. Previous findings suggest that mGluR1α labeling is isolated almost entirely to GABAergic neurons (Stinehelfer et al., 2000). This would suggest that these high intensity cells are interneurons. A way in which

this could be tested would be double labeling sections with NeuN, GAD67 or another interneuron marker. GAD67 may not be the best GABAergic cell marker, since it does not label every GABAergic cell (Roper et al., 1999). Our findings support these results as only around eight percent of neurons were GAD67 positive in the cortical regions examined. This is a markedly lower percentage than the 20-30% of cortical neurons proposed by Markram et al. The makers PV, SS and VIP are thought to label around 82% of cortical interneurons (Rudy et al., 2011). The mGluR1α high intensity cells appear to be negative for SS and VIP labeling. They also appear to be non-overlapping with mGluR5-labeled cells, which are mostly PV positive. This suggests that high intensity mGluR1α cells may belong to the 18% of interneurons that do not express these markers. The majority (~80%) of this population of interneurons express reelin (Rudy et al., 2011).

Neurogliaform (NGF) cells are amongst this class of reelin expressing interneurons (Rudy et al., 2011). NGF cells are small ovoid multipolar cells with a 100-200 micron wide dendritic field and an axonal arbor that is twice that size (Druga, 2009; Kawaguchi and Kubota, 1997; Olah et al., 2007). These cells synapse on pyramidal cells as well as various interneurons (Olah et al., 2007). They have been shown to be electrically coupled amongst themselves (NGF to NGF) as well as with other interneuron cell types (Olah et al., 2007). These observations have been made in both rat and human cortex (Olah et al., 2007). NGF cells have the ability to release sufficient GABA for volume transmission within their axonal field; and are thus capable of synchronizing synaptic activity across distances around 200 microns (Olah et al., 2009). An increase in NGF cells within the PMZ could account for increased or novel avenues for synchronized cortical activity in the malformed brain.

NGF cells have been shown to be reliant on cortical activity prior to P3 for proper cortical migration (De Marco Garcia et al., 2011). Reduced activity was shown to result in NGF cells failing to migrate to the proper location in superficial layers. They were shown to settle in deeper layers than NGF cells found in control cortex (De Marco Garcia et al., 2011). There was also a reduction in the length of the axonal arborizations of these NGF cells as well as in the complexity (not length) of their dendritic trees (De Marco Garcia et al., 2011). This may account for the increase in mGluR1α cells found in the deep layers of the PMZ. However, it would suggest a decrease in the high intensity mGluR1α-labeled cells in the superficial layers of the same region. This was not observed in our counts. There was, however, an increase seen in the percentage of high intensity mGluR1α-labeled cells in superficial layers of the PMZ. This may indicate a compensatory mechanism. There may be a reduction in high intensity mGluR1α-labeled NGF cells in this region due to improper migration that could initiate a compensatory increase in mGluR1α expression within another cell type that ordinarily labels at a lower intensity.

Overall, these studies suggest that the increased physiological response to $mGluR_I$ agonists may in part be due to neurogliaform interneurons that label at a high intensity for mGluR1α. The increase in number of these cells occurs in the PMZ, where the increased physiological responses were observed. The results of this study however cannot account for the increased response to mGluR5 receptors, specifically. Since no change in numbers of mGluR5 cells was observed in the PMZ, these results suggest that instead, an increased number of receptors or intracellular signaling response must account for the physiological findings. Further, in the PMZ, there is no increased expression of mGluR5 in cell types different from those in control cortex. Since the majority of mGluR5 labeling was found in the PV interneuron subtype, this subtype may

participate in the increased responsiveness of PMZ cortex to $mGluR_I$ agonists. It is also possible that SS cells participate, since ~20% of mGluR5 labeled cells did not stain for either PV or VIP, leaving SS as the other major interneuron subtype. Further experiments are necessary to verify physiologically which subtype is responding to the mGluR5 activation as well as to determine the cellular type of the high intensity mGluR1α-labeled cells.

List of References

Araujo D, de Araujo DB, Pontes-Neto OM, Escorsi-Rosset S, Simao GN, Wichert-Ana L, Velasco TR, Sakamoto AC, Leite JP, Santos AC (2006) Language and motor FMRI activation in polymicrogyric cortex. **Epilepsia**, 47: 589-592.

Ascoli GA, Alonso-Nanclares L, Anderson SA, Barrionuevo G, Benavides-Piccione R, Burkhalter A, Buzsaki G, Cauli B, DeFelipe J, Fairen A, Feldmeyer D, Fishell G, Fregnac Y, Freund TF, Gardner D, Gardner EP, Goldberg JH, Helmstaedter M, Hestrin S, Karube F, Kisvarday ZF, Lambolez B, Lewis DA, Marin O, Markram H, Munoz A, Packer A, Petersen CC, Rockland KS, Rossier J, Rudy B, Somogyi P, Staiger JF, Tamas G, Thomson AM, Toledo-Rodriguez M, Wang Y, West DC, Yuste R (2008) Petilla terminology: nomenclature of features of GABAergic interneurons of the cerebral cortex. **Nat Rev Neurosci**, 9: 557-568.

Ballester-Rosado CJ, Albright MJ, Wu CS, Liao CC, Zhu J, Xu J, Lee LJ, Lu HC (2010) mGluR5 in cortical excitatory neurons exerts both cell-autonomous and -nonautonomous influences on cortical somatosensory circuit formation. **J Neurosci**, 30: 16896-16909.

Barkovich AJ (2010) Current concepts of polymicrogyria. **Neuroradiology**, 52: 479-487.

Baskys A, Bayazitov I, Fang L, Blaabjerg M, Poulsen FR, Zimmer J (2005) Group I metabotropic glutamate receptors reduce excitotoxic injury and may facilitate neurogenesis. **Neuropharmacology**, 49 Suppl 1: 146-156.

Bear MF, Huber KM, Warren ST (2004) The mGluR theory of fragile X mental retardation. **Trends Neurosci**, 27: 370-377.

Beck H, Elger CE (2008) Epilepsy research: a window onto function to and dysfunction of the human brain. **Dialogues Clin Neurosci**, 10: 7-15.

Beierlein M, Gibson JR, Connors BW (2000) A network of electrically coupled interneurons drives synchronized inhibition in neocortex. **Nat Neurosci**, 3: 904-910.

Benarroch EE (2008) Metabotropic glutamate receptors: synaptic modulators and therapeutic targets for neurologic disease. **Neurology**, 70: 964-968.

Blumcke I, Vinters HV, Armstrong D, Aronica E, Thom M, Spreafico R (2009) Malformations of cortical development and epilepsies: neuropathological findings with emphasis on focal cortical dysplasia. **Epileptic Disord**, 11: 181-193.

Borowicz KK, Luszczki JJ, Czuczwar SJ (2009) 2-Methyl-6-phenylethynyl-pyridine (MPEP), a non-competitive mGluR5 antagonist, differentially affects the anticonvulsant activity of four conventional antiepileptic drugs against amygdala-kindled seizures in rats. **Pharmacol Rep**, 61: 621-630.

Chassoux F, Landre E, Rodrigo S, Beuvon F, Turak B, Semah F, Devaux B (2008) Intralesional recordings and epileptogenic zone in focal polymicrogyria. **Epilepsia**, 49: 51-64.

De Marco Garcia NV, Karayannis T, Fishell G (2011) Neuronal activity is required for the development of specific cortical interneuron subtypes. **Nature**, 472: 351-355.

Deng W, Wang H, Rosenberg PA, Volpe JJ, Jensen FE (2004) Role of metabotropic glutamate receptors in oligodendrocyte excitotoxicity and oxidative stress. **Proc Natl Acad Sci U S A**, 101: 7751-7756.

Dichter MA, Ayala GF (1987) Cellular mechanisms of epilepsy: a status report. **Science**, 237: 157-164.

Druga R (2009) Neocortical inhibitory system. **Folia Biol (Praha)**, 55: 201-217.

Dvorak K, Feit J (1977) Migration of neuroblasts through partial necrosis of the cerebral cortex in newborn rats-contribution to the problems of morphological development and developmental period of cerebral microgyria. Histological and autoradiographical study. **Acta Neuropathol**, 38: 203-212.

Dvorak K, Feit J, Jurankova Z (1978) Experimentally induced focal microgyria and status verrucosus deformis in rats--pathogenesis and interrelation. Histological and autoradiographical study. **Acta Neuropathol**, 44: 121-129.

Ferraguti F, Conquet F, Corti C, Grandes P, Kuhn R, Knopfel T (1998) Immunohistochemical localization of the mGluR1beta metabotropic glutamate receptor in the adult rodent forebrain: evidence for a differential distribution of mGluR1 splice variants. **J Comp Neurol**, 400: 391-407.

George AL, Jacobs KM (2011) Altered intrinsic properties of neuronal subtypes in malformed epileptogenic cortex. **Brain Res**, 1374: 116-128.

Gibson JR, Beierlein M, Connors BW (1999) Two networks of electrically coupled inhibitory neurons in neocortex. **Nature**, 402: 75-79.

Gobel W, Helmchen F (2007) In vivo calcium imaging of neural network function. **Physiology (Bethesda)**, 22: 358-365.

Guerrini R, Carrozzo R (2002) Epileptogenic brain malformations: clinical presentation, malformative patterns and indications for genetic testing. **Seizure**, 11 Suppl A: 532-543.

Guerrini R, Filippi T (2005) Neuronal migration disorders, genetics, and epileptogenesis. **J Child Neurol**, 20: 287-299.

Huber KM, Gallagher SM, Warren ST, Bear MF (2002) Altered synaptic plasticity in a mouse model of fragile X mental retardation. **Proc Natl Acad Sci U S A**, 99: 7746-7750.

Humphreys P, Rosen GD, Press DM, Sherman GF, Galaburda AM (1991) Freezing lesions of the developing rat brain: a model for cerebrocortical microgyria. **J Neuropathol Exp Neurol**, 50: 145-160.

Jacobs KM, Gutnick MJ, Prince DA (1996) Hyperexcitability in a model of cortical maldevelopment. **Cereb Cortex**, 6: 514-523.

Jacobs KM, Hwang BJ, Prince DA (1999a) Focal epileptogenesis in a rat model of polymicrogyria. **J Neurophysiol**, 81: 159-173.

Jacobs KM, Mogensen M, Warren E, Prince DA (1999b) Experimental microgyri disrupt the barrel field pattern in rat somatosensory cortex. **Cereb Cortex**, 9: 733-744.

Jacobs KM, Prince DA (2005) Excitatory and inhibitory postsynaptic currents in a rat model of epileptogenic microgyria. **J Neurophysiol**, 93: 687-696.

Kawaguchi Y (1993) Groupings of nonpyramidal and pyramidal cells with specific physiological and morphological characteristics in rat frontal cortex. **J Neurophysiol**, 69: 416-431.

Kawaguchi Y, Kondo S (2002) Parvalbumin, somatostatin and cholecystokinin as chemical markers for specific GABAergic interneuron types in the rat frontal cortex. **J Neurocytol**, 31: 277-287.

Kawaguchi Y, Kubota Y (1993) Correlation of physiological subgroupings of nonpyramidal cells with parvalbumin- and calbindinD28k-immunoreactive neurons in layer V of rat frontal cortex. **J Neurophysiol**, 70: 387-396.

Kawaguchi Y, Kubota Y (1997) GABAergic cell subtypes and their synaptic connections in rat frontal cortex. **Cereb Cortex**, 7: 476-486.

Kerner JA, Standaert DG, Penney JB, Jr., Young AB, Landwehrmeyer GB (1997) Expression of group one metabotropic glutamate receptor subunit mRNAs in neurochemically identified neurons in the rat neostriatum, neocortex, and hippocampus. **Brain Res Mol Brain Res**, 48: 259-269.

Kwan P, Brodie MJ (2006) Combination therapy in epilepsy: when and what to use. **Drugs**, 66: 1817-1829.

Long MA, Cruikshank SJ, Jutras MJ, Connors BW (2005) Abrupt maturation of a spike-synchronizing mechanism in neocortex. **J Neurosci**, 25: 7309-7316.

Lujan R (2004) Electron microscopic studies of receptor localization. **Methods Mol Biol**, 259: 123-136.

Marin O (2012) Interneuron dysfunction in psychiatric disorders. **Nat Rev Neurosci**, 13: 107-120.

Markram H, Toledo-Rodriguez M, Wang Y, Gupta A, Silberberg G, Wu C (2004) Interneurons of the neocortical inhibitory system. **Nat Rev Neurosci**, 5: 793-807.

Mellentin C, Moller M, Jahnsen H (2006) Properties of long-term synaptic plasticity and metaplasticity in organotypic slice cultures of rat hippocampus. **Exp Brain Res**, 170: 522-531.

Montenegro MA, Guerreiro MM, Lopes-Cendes I, Guerreiro CA, Cendes F (2002) Interrelationship of genetics and prenatal injury in the genesis of malformations of cortical development. **Arch Neurol**, 59: 1147-1153.

Mudo G, Trovato-Salinaro A, Caniglia G, Cheng Q, Condorelli DF (2007) Cellular localization of mGluR3 and mGluR5 mRNAs in normal and injured rat brain. **Brain Res**, 1149: 1-13.

Neyman S, Manahan-Vaughan D (2008) Metabotropic glutamate receptor 1 (mGluR1) and 5 (mGluR5) regulate late phases of LTP and LTD in the hippocampal CA1 region in vitro. **Eur J Neurosci**, 27: 1345-1352.

Olah S, Fule M, Komlosi G, Varga C, Baldi R, Barzo P, Tamas G (2009) Regulation of cortical microcircuits by unitary GABA-mediated volume transmission. **Nature**, 461: 1278-1281.

Olah S, Komlosi G, Szabadics J, Varga C, Toth E, Barzo P, Tamas G (2007) Output of neurogliaform cells to various neuron types in the human and rat cerebral cortex. **Front Neural Circuits**, 1: 4.

Patrick SL, Connors BW, Landisman CE (2006) Developmental changes in somatostatin-positive interneurons in a freeze-lesion model of epilepsy. **Epilepsy Res**, 70: 161-171.

Pin JP, Bockaert J (1995) Get receptive to metabotropic glutamate receptors. **Curr Opin Neurobiol**, 5: 342-349.

Prince DA, Jacobs KM, Salin PA, Hoffman S, Parada I (1997) Chronic focal neocortical epileptogenesis: does disinhibition play a role? **Can J Physiol Pharmacol**, 75: 500-507.

Rakic P, Lombroso PJ (1998) Development of the cerebral cortex: I. Forming the cortical structure. **J Am Acad Child Adolesc Psychiatry**, 37: 116-117.

Roper SN, Eisenschenk S, King MA (1999) Reduced density of parvalbumin- and calbindin D28-immunoreactive neurons in experimental cortical dysplasia. **Epilepsy Res**, 37: 63-71.

Rosen GD, Jacobs KM, Prince DA (1998) Effects of neonatal freeze lesions on expression of parvalbumin in rat neocortex. **Cereb Cortex**, 8: 753-761.

Rosen GD, Sherman GF, Galaburda AM (1996) Birthdates of neurons in induced microgyria. **Brain Res**, 727: 71-78.

Rudy B, Fishell G, Lee S, Hjerling-Leffler J (2011) Three groups of interneurons account for nearly 100% of neocortical GABAergic neurons. **Dev Neurobiol**, 71: 45-61.

Schwarz P, Stichel CC, Luhmann HJ (2000) Characterization of neuronal migration disorders in neocortical structures: loss or preservation of inhibitory interneurons? **Epilepsia**, 41: 781-787.

Sisodiya SM (2000) Surgery for malformations of cortical development causing epilepsy. **Brain**, 123 (Pt 6): 1075-1091.

Sisodiya SM (2004) Malformations of cortical development: burdens and insights from important causes of human epilepsy. **Lancet Neurol**, 3: 29-38.

Stinehelfer S, Vruwink M, Burette A (2000) Immunolocalization of mGluR1alpha in specific populations of local circuit neurons in the cerebral cortex. **Brain Res**, 861: 37-44.

Tang FR, Bradford HF, Ling EA (2009) Metabotropic glutamate receptors in the control of neuronal activity and as targets for development of anti-epileptogenic drugs. **Curr Med Chem**, 16: 2189-2204.

Weiler IJ, Irwin SA, Klintsova AY, Spencer CM, Brazelton AD, Miyashiro K, Comery TA, Patel B, Eberwine J, Greenough WT (1997) Fragile X mental retardation protein is translated near synapses in response to neurotransmitter activation. **Proc Natl Acad Sci U S A**, 94: 5395-5400.

Wijetunge LS, Till SM, Gillingwater TH, Ingham CA, Kind PC (2008) mGluR5 regulates glutamate-dependent development of the mouse somatosensory cortex. **J Neurosci**, 28: 13028-13037.

World Federation of Neurology, World Health Organization, Dept.of Mental Health and Substance Abuse (2005) **Atlas**
epilepsy care in the world. Geneva: World Health Organization.

Xu W, Wong TP, Chery N, Gaertner T, Wang YT, Baudry M (2007) Calpain-mediated mGluR1alpha truncation: a key step in excitotoxicity. **Neuron**, 53: 399-412.

Zhou M, Xu W, Liao G, Bi X, Baudry M (2009) Neuroprotection against neonatal hypoxia/ischemia-induced cerebral cell death by prevention of calpain-mediated mGluR1alpha truncation. **Exp Neurol**, 218: 75-82.

Vita

William Mark Bruch III was born in Richmond Virginia September 26th 1986. He graduated from Collegiate High School in 2005. He received his Bachelor of Science from Wake Forest University in 2009. He received a Post Baccalaureate Certificate from Virginia Commonwealth University School of Medicine in Premedical Health Sciences in 2010.